Inorganica Chimica Acta, *158* (1989) 81–98

Synthesis and Structure of some Di-iron α-Diimine Complexes Containing a Ferracyclopentadienyl System Resulting from the C–C Coupling of Two Alkynes*

FRED MULLER, INGVILD M. HAN, GERARD VAN KOTEN, KEES VRIEZE**

Laboratorium voor Anorganische Chemie, University of Amsterdam, J.H. van 't Hoff Instituut, Nieuwe Achtergracht 166, 1018 WV, Amsterdam, The Netherlands

DICK HEIJDENRIJK, ROELAND L. DE JONG and MARTIN C. ZOUTBERG

Laboratorium voor Kristallografie, University of Amsterdam, J.H. van 't Hoff Instituut, Nieuwe Achtergracht 166, 1018 WV, Amsterdam, The Netherlands

(Received August 11, 1988)

Abstract

The dinuclear α-diimine complexes $Fe_2(CO)_6(L)$ [L = R-DAB (RN=CHCH=NR, R = i-Pr (**1a**), c-Hex (**1b**)), i-Pr-Pyca (C_5H_4N–CH=N–i-Pr)(**1c**)] react with two equivalents of alkyne R′C≡CR″ [R′ = H, R″ = C(O)OMe, Ph, *p*-Tol, CMe_2OH; R′ = R″ = H, C(O)OMe, Ph], probably via $Fe_2(CO)_5(\sigma,\sigma\text{-}N,N'\text{-L})[\mu_2,\eta^2\text{-}R'C{\equiv}CR'']$, to give various amounts of different isomers of $Fe_2[C_4R'_2R''_2](CO)_4(\sigma,\sigma\text{-}N,N'\text{-L})$. These complexes have a ferracyclopentadienyl fragment $FeC_4R'_2R''_2$ and a chelating 4e donating α-diimine coordinated to the Fe atom bonded to the FeC_4 ferracycle (**3**) or to the Fe atom within the ferracycle (**4**). Fe_2[HC=CHCH=CH]$(CO)_4$(i-Pr-DAB) (**5**) is formed in the thermal reaction of **1a** with ethyne and also has the α-diimine bonded to the Fe within the ferracycle. The product distribution of the reactions seems to depend mainly on steric requirements of the alkyne substituents. In some of the reactions small amounts of alkyne cyclotrimerization products were formed. The X-ray crystal structures of Fe_2[PhC=C(H)C(H)=CPh]$(CO)_4(\sigma,\sigma\text{-}N,N'$-c-Hex-DAB) (**3a**), Fe_2[MeOC(O)C=C(H)C(C(O)OMe)=CH]$(CO)_4(\sigma,\sigma\text{-}N,N'$-i-Pr-DAB) (**3h**), Fe_2[MeOC(O)C=C(C(O)OMe)C(C(O)OMe)=CC(O)OMe]$(CO)_4(\sigma,\sigma\text{-}N,N'$-i-Pr-DAB) (**4e**) and Fe_2[HC=C(H)C(H)=CH]$(CO)_4(\sigma,\sigma\text{-}N,N'$-i-Pr-DAB) (**5**) were determined. (**3a** ($Fe_2C_{34}H_{36}N_2O_4$): orthorhombic crystals, space group *Pbca*, a = 17.353(3), b = 22.814(6), c = 15.911(4) Å, Z = 8, R = 0.070 for 1238 observed reflections. **3h** ($Fe_2C_{20}H_{24}N_2O_8$): monoclinic crystals, space group C_2/c, a = 29.609(5), b = 9.969(2), c = 19.611(3) Å, β = 127.08(1)°, Z = 8, R = 0.064 for 1804 observed reflections. **4e** ($Fe_2C_{24}H_{28}N_2O_{12}$): monoclinic crystals, space group $P2_1/a$, a = 18.287(4), b = 17.966(6), c = 9.002(3) Å, β = 98.96(3)°, Z = 4, R = 0.076 for 1701 observed reflections. **5** ($Fe_2C_{16}H_{20}N_2O_4$): triclinic crystals, space group $P\bar{1}$, a = 9.8291(16), b = 12.1898(22), c = 9.0322(12) Å, α = 111.269(11)°, β = 115.626(19)°, γ = 79.987(23)°, Z = 2, R = 0.046 for 3758 observed reflections.) The complexes **4** contain a bridging CO which makes them the first ferracyclopentadienyl complexes with a bridging CO. The complexes **3** and **5** contain a semi-bridging CO. This coordination behaviour is mainly due to electronic effects. The ^{1}H NMR spectra of the type **3** complexes with two tail-to-tail coupled alkynes show a dynamic behaviour in solution involving the back and forth rocking of the Fe(CO)(α-diimine) fragment with respect to the $Fe(C_4R_4)(CO)_3$ ferracyclopentadienyl fragment.

Introduction

Reactions of metal carbonyl complexes with α-diimines have in the past years resulted in a very extensive chemistry [2]. The α-diimines show a versatile coordination behaviour and it has been found that the coordinated α-diimine ligand may easily participate in not only C–H [3] and N–H [4] bond formation, but also in C–C and N–C coupling reactions with a wide variety of unsaturated organic substrates, such as α-diimines [5], carbodiimides (RN=C=NR) [6], sulphines (R_2C=S=O) [6], ketene (H_2C=C=O) [7] and alkynes (R′C≡CR″) [8].

Of these reactions in particular those involving $Ru_2(CO)_6$(R-DAB) [R-DAB = 1,4-DiAza-1,3-Butadiene: RN=CHCH=NR] containing a 6e donating σ-N,μ_2-N′,η^2-C=N′ coordinated α-diimine ligand have been studied extensively. It has become clear now that in the case of reactions of alkynes with these Ru complexes C–C bond formation between one of the unsaturated C atoms of the alkyne and the η^2-C=N bonded moiety of the R-DAB ligand is the predominant reaction [8a].

---

*Reactions of Dinuclear Metal Carbonyl α-Diimine Complexes with Alkynes, Part 4. For Part 3 see ref. 1.

**Author to whom correspondence should be addressed.

0020-1693/89/$3.50

In order to investigate in more depth the scope and the mechanisms of the reactions of metal carbonyl α-diimine complexes with alkynes we directed our attention to a detailed study of reactions of $M_2(CO)_6$(α-diimine) complexes [M_2 = Ru_2, FeRu, Fe_2; α-diimine = R-DAB, R-Pyca (= pyridine-2-carbaldimine)] with a variety of alkynes.

It has appeared that the reactions of the complexes $Fe_2(CO)_6(L)$ (L = R-DAB, R-Pyca), which are isostructural to $Ru_2(CO)_6$(R-DAB), with different alkynes has resulted in a very extensive and complicated chemistry [8b]. We now report some products of a series of reactions of the complexes $Fe_2(CO)_6(L)$ [L = R-DAB (R = i-Pr, c-Hex) [5c,9], i-Pr-Pyca [5d] with various non-, mono- and disubstituted alkynes. In these products no coupling reactions of the alkyne with the α-diimine ligand have occurred but instead two alkynes are C–C coupled in a similar fashion as in the well known $M_2[C_4R_4](CO)_6$ metallacyclopentadienyl Fe complexes [10]. These complexes are generally regarded as important intermediates in catalytic and stoichiometric oligomerization reactions of alkynes [11]. In the presently reported reactions various types of dinuclear ferracyclopentadienyl α-diimine complexes are formed. The formation and structure of these complexes as well as the bonding in the complexes and the factors determining the product distribution are discussed.

Experimental

Materials and Apparatus

^{1}H and ^{13}C NMR spectra were recorded on Bruker AC100 and WM250 spectrometers. IR spectra were measured with a Perkin-Elmer 283 spectrometer. FD-mass spectra were obtained on a Varian MAT711 double focussing mass spectrometer, fitted with a 10 μm tungsten wire FD-emitter containing carbon microneedles with an average length of 30 μm, using emitter currents of 0–10 mA. UV spectra were recorded in benzene solution on a Perkin-Elmer Lambda 5 UV–Vis Spectrophotometer. Resonance Raman spectra were measured in benzene solution on a Jobin Yvon HG2S Ramanor spectrophotometer. For excitation a SP model 171 argon-ion laser was used. Elemental analyses were carried out by the section Elemental Analysis of the Institute for Applied Chemistry, TNO, Zeist, The Netherlands.

All preparations were carried out in an atmosphere of purified nitrogen, using carefully dried solvents. All column chromatography was performed using silicagel (60 Mesh, dried and activated before use) as the stationary phase. $Fe_2(CO)_6$(R-DAB) [R = i-Pr, c-Hex] [5c] and $Fe_2(CO)_6$(i-Pr-Pyca) [5d] were prepared according to known procedures. Methyl propynoate (MP), phenyl-acetylene (PHA), diphenyl-acetylene (DPHA), ethyne and dimethyl acetylenedicarboxylate (DMADC) were used as commercially obtained. 3-Hydroxy-3-methyl-1-butyne (HMB) was distilled prior to use. Para-tolylacetylene (PTA) was prepared according to literature methods [12]. The obtained products were identified by ^{1}H NMR (Table 1), ^{13}C NMR (Table 2), IR (ν_sC=O) and mass spectroscopy and elemental analyses (Table 3).

Reaction of $Fe_2(CO)_6$(i-Pr-DAB) (1a) with DMADC

Method A. **1a** (1 mmol, 420 mg) and DMADC (1 mmol, 142 mg) were stirred in 50 ml of hexane at 20 °C under reduced pressure for 18 h. The obtained purple suspension was evaporated to dryness and the crude reaction mixture was separated by column chromatography. Elution with hexane/diethyl ether (1:1) afforded the purple compound $Fe_2(CO)_5(\sigma,\sigma\text{-}N,N'$-i-Pr-DAB)[$\mu_2,\eta^2$-MeOC(O)C≡CC(O)OMe] (**2**) in 75–80% yield. Crystallization from hexane/diethyl ether (1:4) at −30 °C produced dark purple crystals suitable for X-ray crystallography [13].

Method B. **1a** (1 mmol, 420 mg) and DMADC (3 mmol, 426 mg) were refluxed in 50 ml of hexane for 4 h. The crude reaction mixture was evaporated to dyness, dissolved in 5 ml of dichloromethane and separated by column chromatography. Elution with hexane/diethyl ether (1:4) and pure diethyl ether yielded minor amounts of a green and a red compound, respectively, which were both as yet unidentified. Elution with diethyl ether/CH_2Cl_2 (4:1) afforded the brown complex Fe_2[MeOC(O)C=C(C(O)OMe)C(C(O)OMe)=CC(O)OMe]$(CO)_4$(i-Pr-DAB) (**4e**) (yield: 70% based on **1a**). Recrystallization from diethyl ether/CH_2Cl_2 (4:1) at −80 °C produced brown crystals suitable for X-ray crystallography.

Reactions of $Fe_2(CO)_5(\sigma,\sigma\text{-}N,N'$-i-Pr-DAB)[$\mu_2,\eta^2$-MeOC(O)C≡CC(O)OMe] (2) with Dimethyl Acetylenedicarboxylate (DMADC) and Methyl Propynoate (MP)

With DMADC. **2** (0.5 mmol, 267 mg) and DMADC (0.5 mmol, 71 mg) were refluxed in hexane for 2 h. After evaporation of the solvent the crude reaction product was purified by column chromatography. Complex **4e** (see above) was obtained by elution with diethyl ether/CH_2Cl_2 (4:1) as a brown fraction in 75% yield.

With MP. **2** (0.5 mmol, 267 mg) and MP (1 mmol, 84 mg) were dissolved in 50 ml of diethyl ether and stirred at 20 °C for four days. The obtained brown solution was evaporated to dryness. Column chromatography of the crude product afforded a small amount of **2** (eluent: hexane/diethyl ether (1:1)). Elution with diethyl ether produced a brown fraction containing the complex Fe_2[MeOC(O)C=C(C(O)OMe)C(H)=CC(O)OMe]$(CO)_4$(i-Pr-DAB) (**4f**) in about 60% yield.

TABLE 1. ^{1}H NMR Data of Fe_2(RC=CR'CR''=CR'''](CO)$_4$(L)[a]

	L[b]	R,R',R'',R'''	i-PrMe[c]	i-PrCH[d]	Pyridine	N=CH	Alkyne
3a[e]	I	Ph,H,H,Ph	1.5(m), 2.8(m)[f]			7.82	6.64(s), 7.2(m), 7.5(m)
3c	II	Ph,H,H,Ph	1.17	3.41		7.95	6.60(s), 7.2(m), 7.5(m)
3d	II	*p*-Tol,H,*p*-Tol	1.17	3.42		7.94	6.56(s), 7.04, 7.38(d,d), 2.29(s)
3e[e]	II	CMe_2OH,H,H,CMe_2OH	1.32/1.37	4.61		7.92	6.14(s), 1.44, 1.55(s,s)
3f	II	CMe_2OH,H,CMe_2OH,H	1.27/1.37, 1.31/1.40	4.03, 4.74		7.84, 8.11	6.35, 7.08(dd, *J* = 3.2 Hz) 1.31, 1.39, 1.45, 1.75(s)
3g	II	C(O)OMe,H,H,C(O)OMe	1.21/1.31	3.67		7.92	7.02(s), 3.74(s)
3h[e]	II	C(O)OMe,H,C(O)OMe,H	1.22/1.23, 1.28/1.42	3.93, 3.94		7.78, 8.09	6.89, 7.84(dd, *J* = 2 Hz) 3.70(s), 3.72(s)
3i	III	C(O)OMe,H,H,C(O)OMe	1.24/1.39	3.98	7–8(m) 8.25(d, 6 Hz)	8.46	6.73, 7.04(dd, *J* = 6 Hz) 3.57(s), 3.85(s)
3j	III	C(O)OMe,H,C(O)OMe,H	1.26/1.42	3.98	7–8(m) 8.22(d, 6 Hz)	8.04	6.69, 7.96(dd, *J* = 3 Hz) 3.71(s), 3.78(s)
3j'	III	C(O)OMe,H,C(O)OMe,H	1.28/1.44	3.98	7–8(m) 8.75(d, 6 Hz)	8.31	6.87, 7.80(dd, *J* = 3 Hz) 3.40(s), 3.54(s)
4a	I	Ph,H,H,Ph	1.5(m), 3–4(m)[f]			7.36, 7.92	6.57, 6.68(dd, *J* = 2 Hz); 7.2(m)
4b[e]	II	Ph,Ph,Ph,Ph	0.67/1.17; 1.55/1.72	4.21, 4.67		7.36, 8.19	6.9(m)
4c	II	Ph,H,H,Ph	0.96/0.99	4.11, 4.48		7.44, 7.95	6.58, 6.69(dd, *J* = 3 Hz); 7.2(m)
4d	II	*p*-Tol,H,H,*p*-Tol	0.96/1.03; 1.37/1.67	4.10, 4.50		7.48, 7.93	6.50, 6.87(dd, *J* = 2 Hz); 2.20(s), 2.26(s), 6.50, 6.78(dd, 7 Hz), 7.00(s)
4e	II	4xC(O)OMe	1.21/1.25, 1.30/1.67	4.05, 4.26		8.09, 8.17	3.41(s), 3.63(s), 3.78(s), 3.81(s)
4f	II	2xC(O)OMe,H,C(O)OMe	1.15/1.21, 1.33/1.71	4.19, 4.25		8.15	6.99(s), 3.46(s), 3.62(s), 3.81(s)
4g	III	4xC(O)OMe	1.30/1.31	4.19	7–8(m) 9.06(d, 6 Hz)	8.38	2.79(s), 3.67(s), 3.78(s), 3.86(s)
4g'[e]	III	4xC(O)OMe	1.42/1.75	4.34	7–8(m) 8.72(d, 6 Hz)	8.30	3.36(s), 3.68(s), 3.72(s), 3.85(s)
4h[e]	III	Ph,Ph,Ph,Ph	1.26/1.73	4.76	7–8(m) 9.26(d, 6 Hz)	8.15	7.0(m)
4h'[e]	III	Ph,Ph,Ph,Ph	0.81/1.65	4.30	7–8(m) 9.11(d, 6 Hz)	7.97	7.0(m)
4l	III	C(O)OMe,H,H,C(O)OMe	1.29/1.31	3.90	7–8(m) 9.42(d, 6 Hz)	8.31	7.15, 7.55(dd, *J* = 3 Hz) 2.81(s), 3.78(s)
4j	III	*p*-Tol,H,H,*p*-Tol	1.00/1.41	4.08	7–8(m)	7.98	6.62, 6.77(dd, 3 Hz); 2.04(s), 2.27(s)
					9.41(d, 6 Hz)		6.13, 6.48(dd, 8 Hz); 7.04(s)
5e	II	H,H,H,H	1.30/1.37	4.25		8.31	6.02, 6.30(dd, dd; *J* = 3.2, 1.2 Hz)

[a] Measured in $CDCl_3$ at 293 K, δ in ppm relative to Me_4Si, spectrometer frequency 100 MHz. [b] I: L = c-Hex-DAB; II: L = i-Pr-DAB; III: L = i-Pr-Pyca. [c] Doublets, *J* = 6 Hz. [d] Septets, *J* = 6 Hz. [e] Spectr. freq. 250 MHz. [f] c-Hex protons.

Reaction of $Fe_2(CO)_6$(i-Pr-DAB) (1a) with Methyl Propynoate (MP)

1a (2 mmol, 840 mg) and MP (6 mmol, 504 mg) were refluxed in 50 ml of heptane for 2 h. The crude reaction mixture was separated by column chromatography. The hexane fraction contains a small amount of $Fe(CO)_3$(i-Pr-DAB) [14]. Elution with hexane/diethyl ethere (4:1) yielded a minor amount of an as yet unidentified yellow product. Further elution produced a faintly purple coloured fraction containing a small amount of an unidentified organometallic compound and small amounts of 1,2,4-tris(methoxycarbonyl)benzene and 1,3,5-tris(methoxycarbonyl)benzene. The next fraction (hexane/diethyl ether (3:2)) contained the brown complex $Fe_2(CO)_4$[i-Pr-NC(H)C(H)N(i-Pr)C(H)=CC(O)OMe] in about 15% yield [1]. Elution with hexane/diethyl ether (1:4) produced the intensely coloured purple

TABLE 2. ^{13}C NMR Data of $Fe_2[RC{=}CR'CR''{=}CR'''](CO)_4(L)$[a]

	L[b]	R,R′,R″,R‴	i-PrMe	i-PrCH	N=CH	C=cc=C	c=CC=c	Alkyne-R	COs
3a[c]	I	Ph,H,H,Ph	24.7, 25.0,	68.4[h]	152.2	159.9	113.9	125.9, 127.5	210.9, 212.6
			34.0, 36.5[h]					127.8, 150.1	231.8
3c[d]	II	Ph,H,H,Ph	24.2, 25.9,	60.5	152.9	163.2	113.9	126–130,	211.4, 231.6
			26.1					151.1	
3d[e]	II	*p*-Tol,H,H,*p*-Tol	21.4, 21.5	60.2	152.7	162.6	113.8	126–149	211.5
								22.3(Me)	
3e[f]	II	CMe_2OH,H,H,CMe_2OH	22.4,26.2	62.0	153.8	n.o.	104.7	32.0, 36.4	n.o.
								79.9(COH)	
3f[f]	II	CMe_2OH,H,CMe_2OH,H	23.6, 24.2	61.1	152.8	154.1	103.2CH	31.4, 31.8, 36.3	204.0, 211.1
			26.2, 26.7	61.9	152.9	163.1(CR)	140.2	73.0, 78.9(COH)	212.6, 212
3g[d]	II	C(O)OMe,H,H,C(O)OMe	23.5, 25.9	61.9	154.2	140.3	115.1	52.3(OMe)	223.0
								176.9C(O)O	
3h[d]	II	C(O)OMe,H,C(O)OMe,H	22.5, 22.6,	62.3	155.3	123.7CR	111.5CR	51.8(OMe)	n.o
			25.5, 25.7		155.5	167.5	115.0	166.6, 176.1(C(O)O)	
4b[d]	II	Ph,Ph,Ph,Ph	21.6, 22.5	57.5	153.8	175.9	139.2	124–152	207.1
			26.2, 26.3	62.3	155.4	178.2	141.8		
4c[c]	II	Ph,H,H,Ph	21.5, 21.8	57.8	153.5	179.9	115.4	124–152	208.4
			25.1, 26.1	61.4	154.0	180.1	117.7		
4d[f]	II	*p*-Tol,H,H,*p*-Tol	21.4, 21.5	58.5	154.5	180.9	116.3	127–150	209.0
			22.3, 22.4	62.0	154.7	181.3	116.6	25.8, 26.8Me	
4e[d]	II	4xC(O)OMe	22.1, 22.7	59.5	156.4	152.2	114.1	51.3, 51.5, 52.6	208.3
			24.2, 26.2	65.0	159.1	162.1	121.1	165.0, 172.2, 175.4	
4f[g]	II	2xC(O)OMe,H,C(O)OMe	22.5, 22.8	60.1	157.0	144.2	109.9CR	52.0, 52.2, 53.0	186.5, 209.5
			24.3, 24.6	64.9	159.1	165.2	116.0	171.1, 172.2, 173.6	213.0
5[c]	II	H,H,H,H	22.6, 24.4	57.8	152.5	157.0	110.2		213.8, 215.6

[a] Measured in $CDCl_3$, δ in ppm relative to Me_4Si. [b] I: L = c-Hex-DAB; II: L = i-Pr-DAB. [c] T = 273 K, SF = 63 MHz. [d] T = 310 K, SF = 20 MHz. [e] T = 293 K, SF = 25 MHz. [f] T = 273 K, SF = 25 MHz. [g] T = 263 K, SF = 25 MHz. [h] c-Hex C atoms.

compound $Fe_2[MeOC(O)C{=}C(H)C(H){=}CC(O)OMe](CO)_4$(i-Pr-DAB) (**3g**) (yield: 25–30%). Finally, using diethyl ether as eluent a second intensely coloured purple fraction was obtained, containing the complex $Fe_2[MeOC(O)C{=}C(H)C(C(O)OMe){=}CH](CO)_4$(i-Pr-DAB) (**3h**) (yield: 30–35%). Recrystallization of **3h** from hexane/diethyl ether (1:2) produced dark purple crystals suitable for X-ray crystallography.

Reaction of $Fe_2(CO)_6$(R-DAB) (1a: R = i-Pr; 1b: R = c-Hex) with R′C≡CH (R′ = Ph, p-Tol)

1a (2 mmol, 840 mg) and R′C≡CH (6 mmol, R′ = Ph: 612 mg; R′ = *p*-Tol: 696 mg) were refluxed in 50 ml of heptane for 20 h. The solvent was evaporated and the reaction mixture separated by column chromatography. Elution with hexane afforded a minor amount of $Fe(CO)_3$(i-Pr-DAB) [14]. Elution with hexane/diethyl ether (19:1) produced an intensely coloured purple solution of $Fe_2[R'C{=}C(H)C(H){=}CR'](CO)_4$(i-Pr-DAB) (**3c**: R′ = Ph; **3d**: R′ = *p*-Tol) with an average yield of 40% based on **1a**. Further elution with hexane/diethyl ether (6:1) yielded the brown complex $Fe_2[R'C{=}C(H)C(H){=}CR'](CO)_4$(i-Pr-DAB) (**4c**: R′ = Ph; **4d**: R′ = *p*-Tol) with an average yield of 30–35%. Recrystallization of both compounds from hexane at −80 °C yielded dark purple and dark brown crystals, respectively.

A similar reaction of **1b** with PHA yielded analogous products **3a** and **4a**. Dark purple crystals suitable for X-ray crystallography of $Fe_2[PhC{=}C(H)C(H){=}CPh](CO)_4$(c-Hex-DAB) (**3a**) were obtained by recrystallization from a hexane solution at −80 °C.

Reaction of $Fe_2(CO)_6$(i-Pr-DAB) (1a) with Ethyne

Through a refluxing solution of **1a** (2 mmol, 840 mg) in 50 ml of heptane a stream of ethyne was passed for 90 min. After evaporating the solvent from the obtained purple suspension the crude product was purified by column chromatography. Elution with hexane/diethyl ether (10:1) yielded (30–40%) the purple complex $Fe_2[HC{=}C(H)C(H){=}CH](CO)_4$(i-Pr-DAB) (**5**). Recrystallization from hexane at −80 °C produced dark purple crystals suitable for X-ray crystallography.

Reaction of $Fe_2(CO)_6$(i-Pr-DAB) (1a) with Diphenyl-acetylene (DPHA)

1a (1 mmol, 420 mg) and DPHA (3 mmol, 534 mg) were refluxed in 50 ml of hexane. The obtained brown suspension was evaporated to dryness. The

TABLE 3. IR, FD-mass and Analytical Data of $Fe_2[RC{=}CR'CR''{=}CR'''](CO)_4(L)$

	L^a	R,R′,R″,R‴	IR^b (ν_s(C=O) (cm^{-1}))	FD-mass obs. (calc.)	Elemental analysis: obs. (calc.) (%)		
					C	H	N
3a	I	Ph,H,H,Ph	2035(s), 1976(s), 1966(s), 1885(m)	648 (648.36)	63.04 (62.99)	5.61 (5.60)	4.30 (4.32)
3c	II	Ph,H,H,Ph	2030(s), 1962(s,b), 1872(m)	568 (568.23)	59.68 (59.18)	5.39 (4.97)	4.70 (4.93)
3d	II	*p*-Tol,H,H,*p*-Tol	2035(s), 1966(s,b), 1878(m)	596 (596.29)	60.43 (60.43)	5.52 (5.41)	4.58 (4.70)
3e	II	CMe_2OH,H,H,CMe_2OH	2028(s), 1958(s,b), 1892(m)	532 (532.20)	49.53 (49.65)	6.04 (6.06)	5.19 (5.26)
3f	II	CMe_2OH,H,CMe_2OH,H	2033(s), 1969(s), 1962(s), 1889(m)	532 (532.20)	50.78 (49.65)	6.49 (6.06)	4.88 (5.26)
3g	II	C(O)OMe,H,H,C(O)OMe	2052(s), 1988(s,b), 1912(m), 1685(m)	532 (532.11)	45.09 (45.14)	4.82 (4.55)	4.99 (5.26)
3h	II	C(O)OMe,H,C(O)OMe,H	2049(s), 1989(s), 1973(s), 1921(m) 1720(m), 1685(m)	532 (532.11)	44.71 (45.14)	4.60 (4.55)	5.01 (5.26)
3i	III	C(O)OMe,H,H,C(O)OMe	2059(s), 2032(m), 1998(s), 1985(s) 1993(m), 1723(w), 1693(w)	540 (540.13)	46.70 (45.25)	3.73 (4.29)	5.19 (4.47)
3j 3j′	III	C(O)OMe,H,C(O)OMe,H	2036(s), 1968(s,b), 1955(sh) 1915(m), 1700(m), 1665(w)	540 (540.13)	not analyzed		
4a	I	Ph,H,H,Ph	1991(s), 1942(s,b), 1794(m)	648 (648.36)	not analyzed		
4b	II	Ph,Ph,Ph,Ph	1988(s), 1954(s), 1924(s), 1794(s)	721 (720.43)	65.31 (66.69)	5.15 (5.04)	3.75 (3.89)
4c	II	Ph,H,H,Ph	1991(s), 1944(s,b), 1794(m)	569 (568.23)	57.56 (59.18)	5.15 (4.97)	4.79 (4.93)
4d	II	*p*-Tol,H,H,*p*-Tol	1987(s), 1941(s,b), 1789(m)	596 (596.29)	60.65 (60.43)	5.60 (5.41)	4.56 (4.70)
4e	II	4xC(O)OMe	2029(s), 1979(s,b), 1844(m) 1722(m), 1695(w)	648 (648.19)	44.15 (44.47)	4.21 (4.35)	4.35 (4.32)
4f	II	2xC(O)OMe,H,C(O)OMe	2020(s), 1974(s,b), 1841(m)	590 (590.15)	44.05 (44.78)	4.52 (4.44)	4.67 (4.75)
4g 4g′	III	4xC(O)OMe	2023(s), 1977(m,b), 1831(m), 1722(m), 1686(m)	656 (656.21)	not analyzed		
4h 4h′	III	Ph,Ph,Ph,Ph	1985(s), 1951(s), 1923(s), 1779(m)	728 (728.45)	not analyzed		
4l	III	C(O)OMe,H,H,C(O)OMe	2008(s), 1960(m), 1811(m), 1708(w) 1673(w)	540 (540.13)	not analyzed		
4j	III	*p*-Tol,H,H,*p*-Tol	1993(s), 1944(s,b), 1783(m)	604 (604.31)	not analyzed		
5	II	H,H,H,H	2021(s), 1972(s), 1934(s), 1892(w)	416 (416.04)	45.84 (46.19)	4.92 (4.85)	6.61 (6.73)

[a] I: L = c-Hex-DAB; II: L = i-Pr-DAB; III: L = i-Pr-Pyca. [b] Type **3** and **5** complexes measured in hexane solution, type **4** complexes measured in dichloromethane solution (s = strong, m = medium, w= weak, b = broad).

product $Fe_2[PhC{=}C(Ph)C(Ph){=}CPh](CO)_4$(i-Pr-DAB) (**4b**) was purified by column chromatography using hexane/diethyl ether (5:1) as the eluent (yield: 70%). Recrystallization from hexane/diethyl ether (1:1) at −20 °C produced brown crystals.

Reaction of $Fe_2(CO)_6$(i-Pr-DAB) (1a) with 3-Hydroxy-3-methyl-1-butyne (HMB)

1a (1 mmol, 420 mg) and HMB (3 mmol, 252 mg) were refluxed in 30 ml of hexane. After 2 h the solvent and the excess of alkyne were evaporated from the obtained purple suspension and the reaction mixture was separated by column chromatography. Elution with hexane yielded a minor amount of $Fe(CO)_3$(i-Pr-DAB) [14]. Further elution with hexane/diethyl ether (4:1) produced a purple fraction containing the complex $Fe_2[HOCMe_2C{=}C(H)C(H){=}CCMe_2OH](CO)_4$(i-Pr-DAB) (**3e**) in 30–35% yield. A second purple fraction was obtained by elution with hexane/diethyl ether (1:1) containing $Fe_2[HOCMe_2C{=}C(H)C(CMe_2OH){=}CH](CO)_4$(i-Pr-DAB) (**3f**) in 40–50% yield.

Reaction of $Fe_2(CO)_6$(i-Pr-Pyca) (1c) with Methyl Propynoate (MP)

1c (1 mmol, 428 mg) and MP (3 mmol, 252 mg) were stirred in 50 ml of hexane at 40 °C. After 26 h the reaction mixture was evaporated to dryness and separated by column chromatography. Elution with hexane/diethyl ether (19:1) afforded a small amount of unreacted **1c**. Further elution with hexane/diethyl ether (4:1) produced a small amount of the as yet structurally uncharacterized complex $Fe_2[C_4H_2(C(O)OMe)_2](CO)_6$ (yield < 5%). Elution with hexane/diethyl ether (2:3) afforded a purple fraction containing the complex $Fe_2[MeOC(O)C{=}C(H)C(H){=}CC(O)OMe](CO)_4$(i-Pr-Pyca) (**3i**) (yield: 5–10%). The next fraction (hexane/diethyl ether (1:4)) yielded a mixture of the two intensely blue–purple coloured compounds $Fe_2[\mu_2\text{-}HC{=}C(C(O)OMe){-}C(O)](CO)_5$(i-Pr-Pyca) and $Fe_2[\mu_2\text{-}MeOC(O)C{=}C(H){-}C(O)](CO)_5$(i-Pr-Pyca) (total yield 40–50%) [15]. Elution with diethyl ether yielded a purple fraction containing a mixture of two isomeric complexes $Fe_2[MeOC(O)C{=}C(H)C(C(O)OMe){=}CH](CO)_4$(i-Pr-Pyca) (**3j**, **3j′**) (average total yield: 20%). Further elution with diethyl ether afforded the brown–red complex $Fe_2[MeOC(O)C{=}C(H)C(H){=}CC(O)OMe](CO)_4$(i-Pr-Pyca) (**4i**) in a yield varying from 10–20%.

Reaction of $Fe_2(CO)_6$(i-Pr-Pyca) (1c) with Dimethyl Acetylenedicarboxylate (DMADC)

1c (1 mmol, 428 mg) and DMADC were stirred in hexane for 28 h at 20 °C. The reaction mixture was evaporated to dryness and separated by column chromatography. The first fraction (diethyl ether/CH_2Cl_2 (9:1)) yielded the dark purple complex $Fe_2[\mu_2\text{-}MeOC(O)C{=}C(C(O)OMe){-}C(O)](CO)_5$(i-Pr-Pyca) in 60–70% yield [15]. Elution with diethyl ether/CH_2Cl_2 (3:2) produced a second fraction containing a 1:2 mixture of two isomeric complexes $Fe_2[MeOC(O)C{=}C(C(O)OMe)C(C(O)OMe){=}CC(O)OMe](CO)_4$(i-Pr-Pyca) (**4g**, **4g′**) in a yield varying from 10–20%.

Reaction of $Fe_2(CO)_6$(i-Pr-Pyca) (1c) with Para-tolyl-acetylene (PTA)

1c (1 mmol, 428 mg) and PTA (3 mmol, 348 mg) were refluxed in 50 ml of hexane for 19 h. After evaporating the solvent the crude product was purified by column chromatography. Elution with hexane afforded a minor amount of 1,2,4-tris(para-tolyl)benzene. Further elution with hexane/diethyl ether (9:1) yielded a small amount of an as yet unidentified organic compound and a minor amount of the as yet structurally uncharacterized purple complex $Fe_2(CO)_4$(i-Pr-Pyca)(p-Tol$C_2H)_2$. Finally, the hexane/diethyl ether (4:1) fraction produced the brown complex $Fe_2[p\text{-}Tol{-}C{=}C(H)C(H){=}C\text{-}p\text{-}Tol](CO)_4$(i-Pr-Pyca) (**4j**) with an average yield of about 20%.

Reaction of $Fe_2(CO)_6$(i-Pr-Pyca) (1c) with Diphenylacetylene (DPHA)

1c (1 mmol, 428 mg) and DPHA (7 mmol, 1246 mg) were refluxed in 50 ml of hexane for 24 h. After evaporation of the solvent the crude reaction mixture was separated by column chromatography. Unreacted DPHA and a small amount of **1c** were obtained by elution with hexane/diethyl ether (9:1). Elution with diethyl ether/CH_2Cl_2 (3:2) yielded a mixture of the two isomeric complexes $Fe_2[PhC{=}C(Ph)C(Ph){=}CPh](CO)_4$(i-Pr-Pyca) (**4h**, **4h′**) in low yield (10–20%).

Crystal Structure Determinations of $Fe_2[PhC{=}C(H)C(H){=}CPh](CO)_4$(c-Hex-DAB) (3a), $Fe_2[MeOC(O)C{=}C(H)C(C(O)OMe){=}CH](CO)_4$(i-Pr-DAB) (3h), $Fe_2[MeOC(O)C{=}C(C(O)OMe)C(C(O)OMe){=}CC(O)OME](CO)_4$(i-Pr-DAB) (4e) and $Fe_2[HC{=}C(H)C(H){=}CH](CO)_4$(i-Pr-DAB) (5)

The crystal and intensity collection data, solution methods and refinement parameters for the three crystal structure determinations are summarized in Table 4. The intensities were measured (θ–2θ scan, 20 °C) on a Nonius CAD4 diffractometer, using graphite monochromated radiation. The structures were all solved by means of the heavy atom method. Refinement proceeded via block-diagonal least-squares calculations. The atomic parameters of the Fe, C, N and O atoms were refined anisotropically, whereas the parameters of the H atoms (if determined, see Table 1) were refined isotropically. An empirical absorption correction was applied (DIFABS) [16] and the anomalous dispersion of Fe was taken into account. The calculations were performed with XRAY76 [17], the atomic scattering factors were taken from Cromer and Mann [18], and the dispersion correction factors from the International Tables for X-Ray Crystallography [19].

Results and Discussion

The complexes $Fe_2(CO)_6(L)$ [L = R-DAB (R = i-Pr, c-Hex); i-Pr-Pyca] (**1a–c**) react with various alkynes $R'C{\equiv}CR''$ to give the dinuclear ferracyclopentadienyl complexes $Fe_2[C_4R'_2R''_2](CO)_4(L)$, formed by the coupling of two alkynes and an Fe center according to eqn. (1).

$$\underset{\mathbf{1a\text{–}c}}{Fe_2(CO)_6(L)} + 2R'C{\equiv}CR'' \longrightarrow \underset{\mathbf{3,\,4,\,5}}{Fe_2[C_4R'_2R''_2](CO)_4(L)} + 2CO \qquad (1)$$

The number of different isomers and the yields in which they are formed strongly vary for the different α-diimines and alkynes (see ‘Experimental’).

TABLE 4. Crystal and Intensity Collection Data, Solution Methods and Refinement Parameters for $Fe_2[PhC{=}CHCH{=}CPh](CO)_4$(c-Hex-DAB) (**3a**), $Fe_2[MeOC(O)C{=}CHC(C(O)OMe){=}CH](CO)_4$(i-Pr-DAB) (**3h**), $Fe_2[MeOC(O)C{=}C(C(O)OMe)C(C(O)OMe{=}CC(O)OMe](CO)_4$(i-Pr-DAB) (**4e**) and $Fe_2[HC{=}C(H)C(H){=}CH](CO)_4$(i-Pr-DAB) (**5**)

	3a	3h	4e	5
Formula	$Fe_2C_{34}H_{36}N_2O_4$	$F_2C_{20}H_{24}N_2O_8$	$Fe_2C_{24}H_{28}N_2O_{12}$	$Fe_2C_{16}H_{20}N_2O_4$
Molecular weight	648.36	532.11	648.19	416.04
Crystal system	orthorhombic	monoclinic	monoclinic	triclinic
Space group	*Pbca*	*C*2/*c*	$P2_1/a$	$P\bar{1}$
$a(\sigma)$ (Å)	17.353(3)	29.609(5)	18.287(4)	9.8291(16)
$b(\sigma)$ (Å)	22.814(6)	9.969(2)	17.966(6)	12.1898(22)
$c(\sigma)$ (Å)	15.911(4)	19.611(3)	9.002(3)	9.0322(12)
$\alpha(\sigma)$ (°)	90.0	90.0	90.0	111.269(11)
$\beta(\sigma)$ (°)	90.0	127.08(1)	98.96(3)	115.626(19)
$\gamma(\sigma)$ (°)	90.0	90.0	90.0	79.987(23)
V (Å^3)	6299.03	4618.13	2921.15	909.1
Z, d_{calc} (g cm^{-3})	8, 1.37	8, 1.53	4, 1.33	2, 1.52
μ (cm^{-1}) (X-rays)	5.14 (Mo Kα)	105.4 (Cu Kα)	10.64 (Mo Kα)	16.15 (Mo Kα)
Crystal colour	dark purple	dark purple	brown	purple
Dimensions (mm)	0.38 × 0.15 × 0.05	0.30 × 0.38 × 0.15	0.23 × 0.08 × 0.13	0.75 × 0.70 × 0.25
h (min, max)	0, 17	−30, 30	−20, 20	−13, 12
k (min, max)	0, 22	−10, 0	0, 20	−17, 15
l (min, max)	0, 15	−20, 0	0, 10	0, 12
2θ range (°)	2.2–44	5.0–110	2.2–50	2.2–60
Total no. reflections	4420	6197	5294	5248
No. reflections $I < 2.5\sigma(I)$	2982	4393	3593	1489
No. reflections in refinement	1238	1804	1701	3758
Fe atoms	E^2-Patterson	symbolic addition[a]	symbolic addition[a]	symbolic addition[a]
C, N, O atoms	ΔF-Fourier	ΔF-Fourier	ΔF-Fourier	ΔF-Fourier
H atoms	excluded	ΔF-Fourier[b]	excluded	ΔF-Fourier
R (R_w)	0.070 (0.114)	0.064 (0.092)	0.076 (–)	0.046 (–)
Extinction correction	yes	no	no	yes
Weighting scheme	$2.86 + F + 0.0157F^2$	$9.22 + F + 0.01047F^2$	unit weights	unit weights

[a] Using the symbolic addition program set SIMPEL [20]. [b] After anisotropic refinement of the F, C, N and O atoms.

In only one case could an intermediate in the formation of the ferracyclopentadienyl complexes be isolated: the reaction of **1a** with DMADC, at room temperature yielded the purple complex $Fe_2(CO)_5(\sigma,\sigma\text{-}N,N'\text{-i-Pr-DAB})[\mu_2,\eta^2\text{-}MeOC(O)C{\equiv}CC(O)OMe]$ (**2**) of which the X-ray crystal structure has been determined [13] (see Scheme 1). This complex (**2**) reacts further with a second equivalent of alkyne (DMADC, MP) to give $Fe_2[MeOC(O)C{=}C(C(O)OMe)C(R'){=}CC(O)OMe](CO)_4$(i-Pr-DAB) (**4e**: R′ = C(O)OMe; **4f**: R′ = H) (see eqn. (2)).

$$Fe_2(CO)_6(\text{i-Pr-DAB})\ (\mathbf{1a}) + \text{DMADC} \longrightarrow$$

$$Fe_2(CO)_5(\text{i-Pr-DAB})[\mu_2,\eta^2\text{-DMADC}]\ (\mathbf{2}) + CO$$

$$\mathbf{2} + RC{\equiv}CC(O)OMe\ (R = H, C(O)OMe) \longrightarrow$$

$$Fe_2[C_4R(C(O)OMe)_3](CO)_4(\text{i-Pr-DAB})\ (\mathbf{4e}, \mathbf{4f}) + CO \qquad (2)$$

The complexes $Fe_2(C_4R'_2R''_2)(CO)_4(L)$ have a number of general features. In all complexes the alkynes are C–C coupled and the resulting butadiendiyl fragment forms with one of the Fe atoms a ferracyclopentadienyl fragment. This ferracycle is bonded to the other Fe center via two π-bonded olefinic bonds as well as via a metal–metal bond. Furthermore, in all complexes the α-diimine ligand L is coordinated in the σ,σ-N,N' chelating 4e donating bonding mode. When L = i-Pr-Pyca, in most reactions an inseparable mixture of the two possible regioisomers with respect to the coordination of the two inequivalent N atoms of the Pyca ligand was obtained.

Apart from these general features the reported compounds can be divided into three different types, which are schematically shown in Fig. 1: In the complexes **3** the α-diimine ligand is coordinated to the Fe center that is bonded to the FeC_4 ferracycle. They thus consist of a ferracyclopentadienyl fragment $Fe(CO)_3(C_4R'_2R''_2)$ bonded to an Fe(CO)(L) unit of which the CO is semi-bridging.

In the complexes **4** the α-diimine ligand is coordinated to the Fe atom in the FeC_4 ferracycle. An important structural difference with the complexes **3** is the presence of a bridging CO ligand instead of a semi-bridging CO. Only complexes of this type (**4**) with two tail-to-tail coupled alkynes were formed.

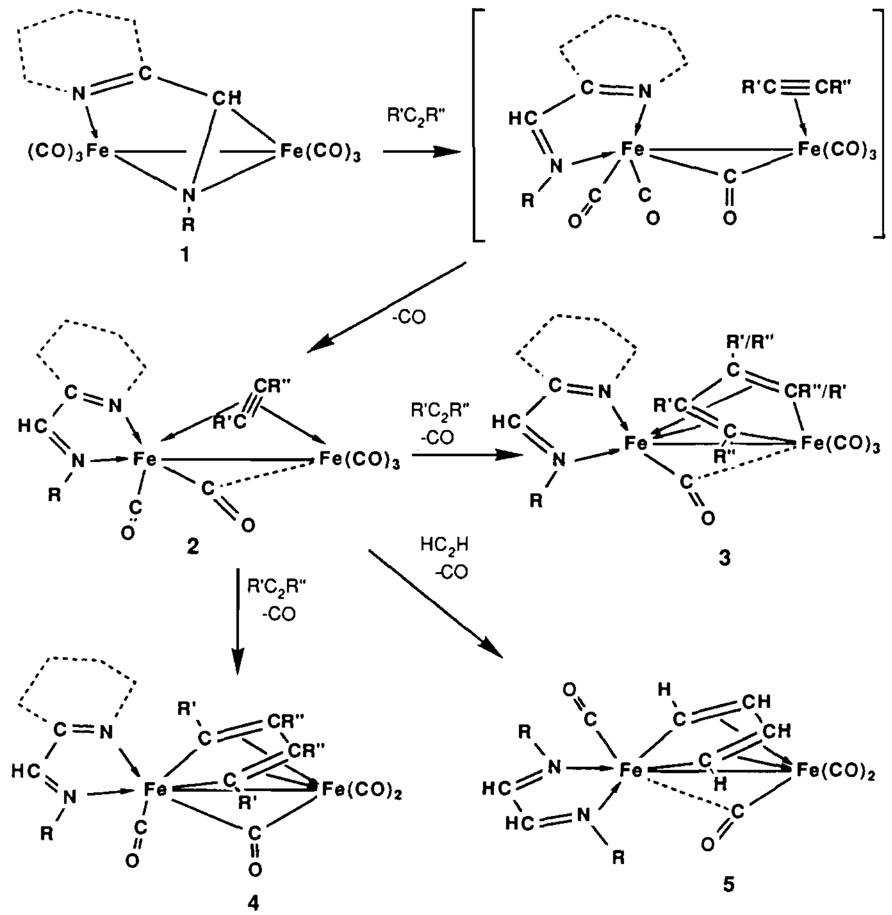

Scheme 1. Proposed mechanism of the formation of 3, 4 and 5 [R = i-Pr, c-Hex; R' = H, R'' = Ph, *p*-Tol, CMe_2OH, C(O)OMe; R' = R'' = H, Ph, C(O)OMe].

In 5 the DAB ligand is also bonded to the Fe in the ferracycle. In this complex, however, the N atoms of the DAB ligand occupy the coordination sites *trans* to the terminal C atoms of the butadiendiyl fragment. This type of complex, which is exclusively found in the reactions of $Fe_2(CO)_6$(R-DAB) with ethyne, contains a semi-bridging CO, in contrast to the bridging CO in the complexes 4 in which the α-diimine is also bonded to the Fe atom in the ferracycle.

The complexes 3 can be regarded as isostructural and isoelectronic with the well-known ferracyclopentadienyl complexes $Fe_2(C_4R_4)(CO)_6$ [10] formed in reactions of Fe carbonyl clusters with alkynes. In the past 25 years a number of crystal structure determinations of complexes of this type have been published, the first one being that of Fe_2(HO–C=C(Me)C(Me)=C–OH]$(CO)_6$ [21]. This compound was also the first structurally characterized complex with a semi-bridging CO ligand. The difference between those complexes and the presently reported complexes 3 is obviously the α-diimine ligand which replaces two terminal COs by the two N donor atoms of the α-diimine ligand. The complexes 3, which result from the reactions of 1 with monosubstituted alkynes, can be further divided into a group of complexes containing two head-to-tail (≡CR to ≡CH) coupled alkynes (e.g. **3h**) and those with two tail-to-tail (≡CH to ≡CH) coupled alkynes (e.g. **3a**). Products containing two head-to-head coupled alkynes are not formed, which is most likely due to steric reasons.

Of each of the complex types 3, 4 and 5 the X-ray single crystal structure of one compound, representative of its type, was determined. The crystal structures of Fe_2[PhC=C(H)C(H)=CPh]$(CO)_4$(c-Hex-DAB) (**3a**), with two tail-to-tail coupled alkynes, Fe_2[MeOC(O)C=C(H)C(C(O)OMe)=CH]$(CO)_4$(i-Pr-DAB) (**3h**), with two head-to-tail coupled alkynes, Fe_2[MeOC(O)C=C(C(O)OMe)C(C(O)OMe)=CC(O)OMe]$(CO)_4$(i-Pr-DAB) (**4e**) and Fe_2[HC=C(H)C(H)=CH]$(CO)_4$(i-Pr-DAB) (**5**) have been determined.

Fractional coordinates of the non-H atoms of **3a**, **3h**, **4e** and **5** are given in Tables 5, 6, 7 and 8 respectively. Table 9 gives their comparable bond lengths.

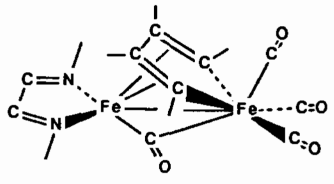

3

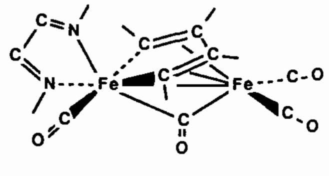

4

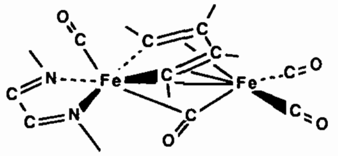

5

Fig. 1. Schematic representation of the product types 3, 4 and 5.

TABLE 5. Fractional Coordinates of the Non-H Atoms of 3a

Atom	*x*	*y*	*z*
Fe(1)	0.0820(2)	0.2593(1)	0.3569(2)
Fe(2)	−0.0074(2)	0.2839(1)	0.4758(2)
C(1)	0.134(1)	0.2612(9)	0.451(1)
C(2)	−0.099(1)	0.3120(8)	0.489(1)
C(3)	0.032(1)	0.3213(9)	0.560(1)
C(4)	−0.011(1)	0.2191(9)	0.536(1)
C(5)	−0.039(1)	0.2449(8)	0.368(1)
C(6)	−0.025(1)	0.2762(8)	0.295(1)
C(7)	0.016(1)	0.3309(9)	0.306(1)
C(8)	0.034(1)	0.3422(8)	0.390(1)
C(9)	−0.088(1)	0.1920(8)	0.360(1)
C(10)	−0.086(1)	0.1582(9)	0.285(1)
C(11)	−0.134(1)	0.1075(10)	0.274(1)
C(12)	−0.182(1)	0.0901(11)	0.342(2)
C(13)	−0.186(1)	0.1226(8)	0.415(1)
C(14)	−0.139(1)	0.1749(9)	0.426(1)
C(15)	0.068(1)	0.4006(9)	0.411(1)
C(16)	0.030(1)	0.4492(9)	0.382(2)
C(17)	0.055(1)	0.5053(10)	0.401(2)
C(18)	0.124(2)	0.5161(10)	0.450(2)
C(19)	0.160(1)	0.4654(9)	0.475(2)
C(20)	0.135(1)	0.4114(9)	0.458(2)
C(21)	0.166(1)	0.1733(10)	0.271(1)
C(22)	0.196(1)	0.2301(8)	0.245(2)
C(23)	0.082(1)	0.1253(8)	0.370(1)
C(24)	0.142(1)	0.1114(10)	0.443(1)
C(25)	0.103(1)	0.0570(9)	0.493(1)
C(26)	0.095(2)	0.0012(10)	0.438(1)
C(27)	0.039(1)	0.0190(8)	0.364(1)
C(28)	0.074(1)	0.0728(9)	0.311(1)
C(29)	0.201(1)	0.3336(9)	0.262(1)
C(30)	0.209(1)	0.3488(12)	0.170(1)
C(31)	0.242(2)	0.4120(10)	0.163(2)
C(32)	0.321(1)	0.4123(10)	0.208(2)
C(33)	0.322(1)	0.3941(11)	0.299(2)
C(34)	0.283(1)	0.3350(10)	0.306(2)
N(1)	0.1113(9)	0.1768(7)	0.329(1)
N(2)	0.1651(9)	0.2744(7)	0.277(1)
O(1)	0.1833(8)	0.2599(6)	0.501(1)
O(2)	−0.1609(9)	0.3307(7)	0.496(1)
O(3)	0.0572(10)	0.3462(7)	0.618(1)
O(4)	−0.0097(11)	0.1781(7)	0.580(1)

TABLE 6. Fractional Coordinates of the Non-H Atoms of **3h**

Atom	*x*	*y*	*z*
Fe(1)	0.11944(6)	0.6715(2)	0.20606(10)
Fe(2)	0.09236(7)	0.4727(2)	0.2564(1)
C(1)	0.1487(5)	0.354(1)	0.3239(7)
C(2)	0.0918(5)	0.516(1)	0.3444(8)
C(3)	0.0345(5)	0.365(1)	0.2029(8)
C(4)	0.1844(5)	0.607(1)	0.2963(7)
C(5)	0.0988(4)	0.4745(10)	0.1621(6)
C(6)	0.0612(4)	0.562(1)	0.0938(7)
C(7)	0.0316(4)	0.650(1)	0.1131(7)
C(8)	0.0474(4)	0.630(1)	0.1959(6)
C(9)	0.1340(5)	0.379(1)	0.1524(7)
C(10)	0.1572(5)	0.722(1)	0.0927(7)
C(11)	0.1605(7)	0.296(2)	0.069(1)
C(12)	−0.0056(4)	0.762(1)	0.0555(7)
C(13)	−0.0442(6)	0.881(1)	−0.0755(8)
C(14)	0.1622(5)	0.899(1)	0.1824(8)
C(15)	0.1520(4)	0.936(1)	0.2416(6)
C(16)	0.1230(6)	0.870(1)	0.3273(8)
C(17)	0.0803(7)	0.984(2)	0.2999(10)
C(18)	0.1804(6)	0.903(2)	0.4155(9)
C(19)	0.2117(7)	0.658(2)	0.136(1)
C(20)	0.1440(9)	0.833(2)	0.026(1)
N(1)	0.1320(4)	0.8426(9)	0.2623(5)
N(2)	0.1475(4)	0.7788(9)	0.1549(5)
O(1)	0.1823(4)	0.279(1)	0.3715(6)
O(2)	0.0899(5)	0.537(1)	0.3999(6)
O(3)	−0.0043(4)	0.294(1)	0.1635(6)
O(4)	0.2300(3)	0.5751(10)	0.3525(6)
O(5)	0.1271(3)	0.3850(9)	0.807(5)
O(6)	0.1668(5)	0.306(1)	0.2070(6)
O(7)	−0.0076(3)	0.7734(9)	−0.0136(5)
O(8)	−0.0294(4)	0.8366(8)	0.0729(6)

The σ,σ-*N,N'* chelating R-DAB ligands in all four complexes have normal Fe–N bond lengths [1.94–2.02 Å], imine bond lengths [1.22–1.36 Å] and central C–C bond lengths [1.41–1.48 Å] for this

TABLE 7. Fractional Coordinates of the Non-H Atoms of **4e**

Atom	*x*	*y*	*z*
Fe(1)	−0.1352(1)	0.2674(1)	0.1423(3)
Fe(2)	−0.0003(1)	0.2817(1)	0.1422(3)
N(1)	−0.2000(7)	0.3593(8)	0.121(1)
N(2)	−0.1988(7)	0.2462(7)	0.291(1)
C(1)	−0.194(1)	0.218(1)	−0.006(2)
C(2)	−0.074(1)	0.302(1)	−0.022(2)
C(3)	0.065(1)	0.239(1)	0.047(2)
C(4)	0.047(1)	0.366(1)	0.133(2)
C(5)	−0.251(1)	0.361(1)	0.209(2)
C(6)	−0.249(1)	0.295(1)	0.307(2)
C(7)	−0.197(1)	0.424(1)	0.016(2)
C(8)	−0.247(1)	0.404(1)	−0.136(3)
C(9)	−0.220(1)	0.499(1)	0.083(3)
C(10)	−0.191(1)	0.177(1)	0.388(2)
C(11)	−0.186(1)	0.196(2)	0.554(3)
C(12)	−0.252(2)	0.123(1)	0.334(3)
C(13)	−0.064(1)	0.188(1)	0.180(2)
C(14)	−0.005(1)	0.195(1)	0.307(2)
C(15)	−0.005(1)	0.264(1)	0.379(2)
C(16)	−0.062(1)	0.313(1)	0.304(2)
C(17)	−0.068(1)	0.117(1)	0.092(2)
C(18)	−0.072(1)	0.059(1)	−0.150(2)
C(19)	0.049(1)	0.133(1)	0.357(2)
C(20)	0.090(1)	0.052(1)	0.561(3)
C(21)	0.056(1)	0.285(1)	0.501(2)
C(22)	0.095(1)	0.365(1)	0.707(2)
C(23)	−0.075(1)	0.388(1)	0.359(2)
C(24)	−0.121(1)	0.455(1)	0.554(3)
O(1)	−0.2282(8)	0.1859(9)	−0.100(2)
O(2)	−0.0852(7)	0.3198(9)	−0.149(2)
O(3)	0.1074(9)	0.2129(10)	−0.024(2)
O(4)	0.0766(9)	0.4230(9)	0.123(2)
O(5)	−0.0815(9)	0.0569(7)	0.147(2)
O(6)	−0.0614(7)	0.1260(7)	−0.051(1)
O(7)	0.0925(7)	0.1072(8)	0.281(1)
O(8)	0.0365(7)	0.1071(7)	0.488(1)
O(9)	0.1135(6)	0.2502(8)	0.527(2)
O(10)	0.0398(8)	0.3434(8)	0.576(2)
O(11)	−0.0540(8)	0.4464(7)	0.313(2)
O(12)	−0.1119(7)	0.3847(7)	0.478(1)

coordination mode [2]. The bond lengths and angles of the terminal CO ligands are as expected, which also applies for the substituents on the DAB ligands and alkynes. The specific structural features of the complexes **3a**, **3h**, **4e** and **5** will be discussed in the following sections.

Molecular Structure of $Fe_2[MeOC(O)C{=}C(C(O)OMe)C(C(O)OMe){=}CC(O)OMe](CO)_4(i\text{-}Pr\text{-}DAB)$ *(4e)*

The molecular structure of **4e** consists of an Fe$(CO)_2$ and an Fe(CO)(i-Pr-DAB) unit which are bridged by an asymmetrically bridging CO and a formally 6e donating butadiendiyl ligand, consisting of the C–C coupled DMADC molecules, forming a ferracycle with the Fe(1) atom to which also the DAB ligand is bonded (see Fig. 2). To our knowledge this is the first ferracyclopentadienyl iron complex containing a bridging CO instead of a semi-bridging

TABLE 8. Fractional Coordinates of the Non-H Atoms of **5**

Atom	*x*	*y*	*z*
Fe(1)	0.31898(7)	0.18293(5)	0.76844(7)
Fe(2)	0.31615(6)	0.31801(5)	1.05755(7)
N(1)	0.4728(3)	0.2713(3)	1.2558(4)
N(2)	0.1859(4)	0.2723(3)	1.1383(4)
C(1)	0.1842(5)	0.0998(4)	0.5649(6)
C(2)	0.4785(5)	0.1108(4)	0.7283(6)
C(3)	0.3182(5)	0.1021(4)	0.8999(6)
C(4)	0.3005(5)	0.4689(4)	1.1298(5)
C(5)	0.4162(5)	0.2255(4)	1.3260(6)
C(6)	0.2577(5)	0.2279(4)	1.2625(6)
C(7)	0.6378(4)	0.2805(4)	1.3207(6)
C(8)	0.7304(6)	0.2102(5)	1.4403(7)
C(9)	0.6762(5)	0.4101(5)	1.4045(7)
C(10)	0.0192(5)	0.2860(5)	1.0722(6)
C(11)	−0.0338(7)	0.3582(7)	1.2094(9)
C(12)	−0.0556(8)	0.1752(7)	0.9794(15)
C(13)	0.4497(5)	0.3299(4)	0.9576(6)
C(14)	0.3774(6)	0.3500(4)	0.7944(6)
C(15)	0.2189(6)	0.3422(4)	0.7240(6)
C(16)	0.1641(5)	0.3159(4)	0.8300(5)
O(1)	0.0979(4)	0.0488(3)	0.4335(5)
O(2)	0.5816(4)	0.0658(4)	0.7005(5)
O(3)	0.3159(5)	0.0312(3)	0.9538(5)
O(4)	0.2889(5)	0.5704(3)	1.1659(5)

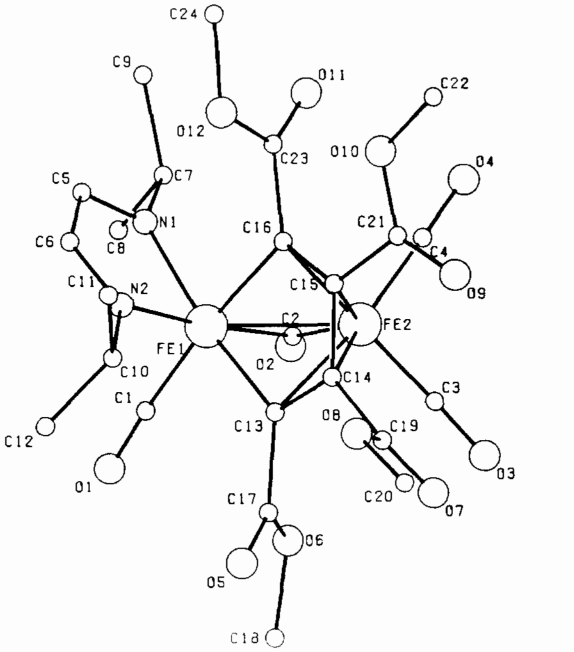

Fig. 2. PLUTO drawing of $Fe_2[MeOC(O)C{=}C(C(O)OMe)C(C(O)OMe){=}CC(O)OMe](CO)_4(i\text{-}Pr\text{-}DAB)$ (**4e**). The H atoms are omitted for clarity.

TABLE 9. Selected Comparable Bond Lengths (Å) in 3a, 3h, 4e and 5[a]

	3a		3h		4e		5	
M–M	Fe(1)–Fe(2)	2.510(3)	Fe(1)–Fe(2)	2.549(2)	Fe(1)–Fe(2)	2.4801(24)	Fe(1)–Fe(2)	2.541(3)
M–N	Fe(1)–N(1)	1.997(14)	Fe(1)–N(1)	1.942(7)	Fe(1)–N(1)	2.024(10)	Fe(2)–N(1)	1.988(4)
	Fe(1)–N(2)	1.974(13)	Fe(1)–N(2)	1.961(8)	Fe(1)–N(2)	1.943(9)	Fe(2)–N(2)	1.958(4)
N=C	N(1)–C(21)	1.359(20)	N(1)–C(15)	1.29(1)	N(1)–C(5)	1.313(17)	N(1)–C(5)	1.301(6)
	N(2)–C(22)	1.221(22)	N(2)–C(14)	1.28(1)	N(2)–C(6)	1.292(16)	N(2)–C(6)	1.294(5)
C–C	C(21)–C(22)	1.46(3)	C(14)–C(15)	1.41(1)	C(5)–C(6)	1.480(19)	C(5)–C(6)	1.407(7)
M–CO	Fe(1)–C(1)	1.755(15)	Fe(1)–C(4)	1.772(9)	Fe(2)–C(2)	1.875(13)	Fe(1)–C(1)	1.780(4)
	Fe(2)...C(1)	2.545(15)	Fe(2)...C(4)	2.70(1)	Fe(1)–C(2)	2.089(13)	Fe(1)–C(2)	1.773(4)
	Fe(2)–C(2)	1.727(16)	Fe(2)–C(1)	1.809(10)	Fe(1)–C(1)	1.802(13)	Fe(1)–C(3)	1.799(4)
	Fe(2)–C(3)	1.718(17)	Fe(2)–C(2)	1.79(1)	Fe(2)–C(3)	1.760(13)	Fe(2)...C(3)	2.501(4)
	Fe(2)–C(4)	1.771(18)	Fe(2)–C(3)	1.74(1)	Fe(2)–C(4)	1.752(15)	Fe(2)–C(4)	1.718(5)
C–O	C(1)–O(1)	1.165(19)	C(4)–O(4)	1.16(1)	C(2)–O(2)	1.176(16)	C(1)–O(1)	1.137(5)
	C(2)–O(2)	1.157(20)	C(1)–O(1)	1.14(1)	C(1)–O(1)	1.136(17)	C(2)–O(2)	1.147(5)
	C(3)–O(3)	1.172(21)	C(2)–O(2)	1.14(1)	C(3)–O(3)	1.166(18)	C(3)–O(3)	1.143(5)
	C(4)–O(4)	1.174(22)	C(3)–O(3)	1.16(1)	C(4)–O(4)	1.169(18)	C(4)–O(4)	1.158(5)
M–C	Fe(2)–C(5)	1.994(14)	Fe(2)–C(5)	1.970(9)	Fe(1)–C(13)	1.916(13)	Fe(2)–C(13)	1.935(5)
	Fe(2)–C(8)	2.024(15)	Fe(2)–C(8)	1.932(8)	Fe(1)–C(16)	1.996(11)	Fe(2)–C(16)	1.944(4)
	Fe(1)–C(5)	2.120(16)	Fe(1)–C(5)	2.083(7)	Fe(2)–C(13)	2.102(13)	Fe(1)–C(13)	2.112(4)
	Fe(1)–C(6)	2.140(14)	Fe(1)–C(6)	2.106(8)	Fe(2)–C(14)	2.164(11)	Fe(1)–C(14)	2.116(4)
	Fe(1)–C(7)	2.123(16)	Fe(1)–C(7)	2.101(10)	Fe(2)–C(15)	2.171(11)	Fe(1)–C(15)	2.111(4)
	Fe(1)–C(8)	2.134(15)	Fe(1)–C(8)	2.06(1)	Fe(2)–C(16)	2.053(11)	Fe(1)–C(16)	2.115(4)
C–C	C(5)–C(6)	1.362(20)	C(5)–C(6)	1.41(1)	C(13)–C(14)	1.445(17)	C(13)–C(14)	1.426(5)
	C(6)–C(7)	1.454(21)	C(6)–C(7)	1.44(1)	C(14)–C(15)	1.407(16)	C(14)–C(15)	1.411(7)
	C(7)–C(8)	1.380(21)	C(7)–C(8)	1.41(1)	C(15)–C(16)	1.449(16)	C(15)–C(16)	1.427(6)

[a] e.s.d.s given in parentheses.

CO or only terminal COs. We assume that the Fe–Fe distance of 2.4801(24) Å is slightly shorter than in other ferracyclopentadienyl complexes, where it is normally in the range of 2.50–2.55 Å [10b], because of this bridging CO ligand. The bonding mode of this CO is asymmetrically bridging since C(2) is significantly closer to Fe(2) than to Fe(1) [Fe(1)–C(2): 2.089(13) Å; Fe(2)–C(2): 1.875(13) Å]. This conclusion is in agreement with the classification criteria for bridging CO ligands formulated by Colton and McCormick [22].

The organic butadiendiyl fragment is also slightly asymmetrically coordinated to the metal carbonyl core as the Fe(1)–C(16) bond length of 1.996(11) Å is significantly longer than the Fe(1)–C(13) distance of 1.916(13) Å. The Fe(2)–C(16) bond length of 2.053(11) Å is also shorter than the Fe(2)–C(13) distance of 2.102(13) Å. The Fe(2)–C(14) and Fe(2)–C(15) distances of 2.164(11) and 2.171(11) Å are almost equal. This asymmetric coordination of the butadiendiyl fragment may satisfactorily be explained by the steric interaction with the coordinated DAB ligand. We can, however, not rule out an electronic *trans* influence, since C(13) is coordinated opposite to a σ-N bonded imine group, whereas C(16) is opposite to a CO ligand.

A striking aspect of this structure concerns the bond lengths within the bridging organic fragment. The bond distances of the formally olefinic bonds C(13)–C(14) [1.445(17) Å] and C(15)–C(16) [1.449(16) Å] show a substantial elongation, while the central C(14)–C(15) distance of 1.407(16) Å is very short for a formally single C–C bond. This equalization of central and terminal C–C bond lengths in dinuclear metallacyclopentadienyl complexes is a generally observed phenomenon and is ascribed to the back-bonding interaction of the organic fragment with the Fe carbonyl core [23]. The extent of delocalization observed in **4e** is, however, rarely observed. This suggests that the bonding of the C_4R_4 fragment must be regarded as intermediate between a ferracyclopentadienyl and a bis(μ_2-alkylidene) structure, with the central C(14)–C(15) bond η^2-C=C bonded to Fe(2). This is supported by the fact that the Fe–C distances of the central C atoms are significantly longer than those of the terminal C atoms of the butadiendiyl fragment. An analogous configuration was also found in a similar complex (η^5-C_5H_5)(CO)Cr(C_4Ph_4)Cr(η^5-C_5H_5) [24]. The deviation of about 0.51 Å of the Cr from the butadiendiyl plane in this complex does not occur in **4e** where Fe(1), C(13), C(14), C(15) and C(16) are almost coplanar (r.m.s. deviation: 0.06 Å).

Molecular Structure of $Fe_2[MeOC(O)C{=}C(H)C(C(O)OMe){=}CH](CO)_4(i\text{-}Pr\text{-}DAB)$ *(3h)*

This structure consists of an $Fe(CO)_3$ and an Fe(CO)(i-Pr-DAB) unit linked by a formally single

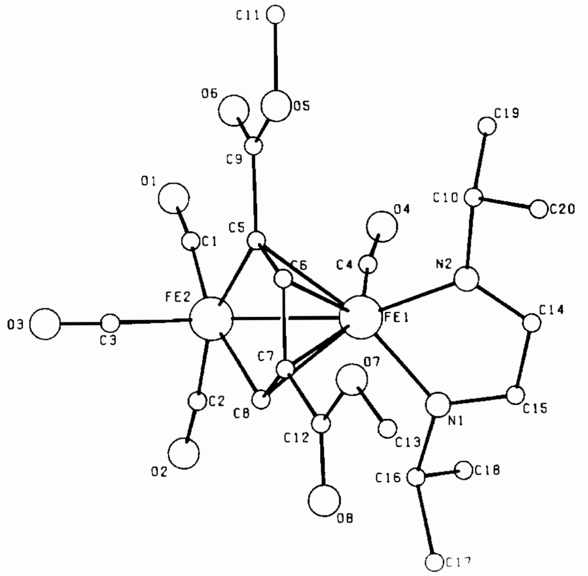

Fig. 3. PLUTO drawing of $Fe_2[MeOC(O)C{=}C(H)C(C(O)OMe){=}CH](CO)_4$(i-Pr-DAB) (**3h**). The H atoms are omitted for clarity.

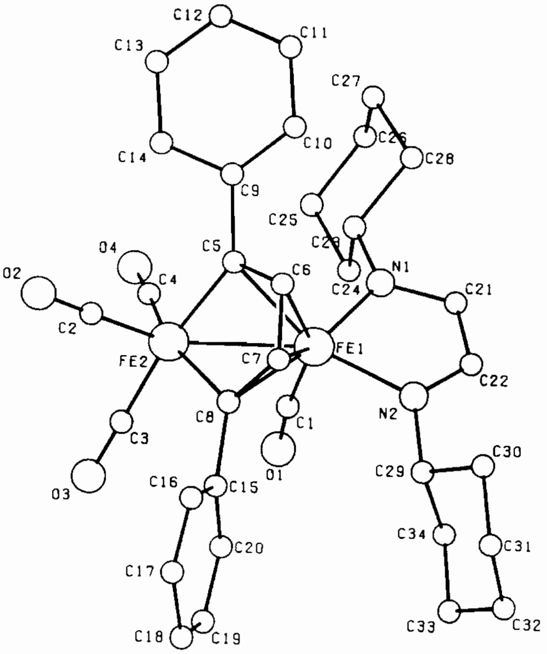

Fig. 4. PLUTO drawing of $Fe_2[PhC{=}C(H)C(H){=}CPh](CO)_4$(c-Hex-DAB) (**3a**).

Fe–Fe bond of 2.549(2) Å that is bridged by a formally 6e donating butadienyl fragment resulting from the head-to-tail coupling of two MP molecules (see Fig. 3). The latter organic fragment forms with Fe(2) a ferracyclopentadienyl fragment that is bonded to the Fe(CO)(i-Pr-DAB) unit. In most of the structurally comparable ferracyclopentadienyl complexes [10b] a semi-bridging CO is present with typical Fe···C distances of 2.35–2.55 Å and an Fe–C–O angle of 160–170°. In **3h**, however, the Fe(2)···C(4) distance of 2.70(1) Å and the Fe(1)–C(4)–O(4) angle of 171.7(7)° suggests that the nature of the bonding of this CO is intermediate between terminal and semi-bridging. The role of the semi-bridging CO in the ferrole complexes and the observed deviation in **3h** is discussed below. Contrary to the asymmetrical bonding mode of the butadiendiyl fragment with respect to the di-iron core in **4e**, it is virtually symmetrically bonded to the metal carbonyl core in **3h** [Fe(2)–C(5): 1.970(9); Fe(2)–C(8): 1.932(8); Fe(1)–C(5): 2.083(7); Fe(1)–C(6): 2.106(8); Fe(1)–C(7): 2.101(10); Fe(1)–C(8): 2.06(1) Å] despite the asymmetric substitution with C(O)OMe groups of the organic fragment itself.

The bonding within this organic fragment also differs significantly from that in 4e. In **3h** the terminal C–C bonds are shorter than the central C(6)–C(7) bond [C(5)–C(6): 1.41(1) and C(7)–C(8): 1.41(1) Å *versus* C(6)–C(7): 1.44(1) Å]. These values are more in agreement with those normally observed in ferrole complexes [10].

Molecular Structure of $Fe_2[PhC{=}C(H)C(H){=}CPh]$-$(CO)_4$(c-Hex-DAB) (3a)

Like **3h** this complex is composed of an $Fe(CO)_3$ unit and an Fe(CO)(c-Hex-DAB) fragment bridged by a butadiendiyl ligand that forms a ferracyclopentadienyl ring with the Fe(2) atom in the $Fe(CO)_3$ fragment (see Figs. 4 and 5). There are, however, a number of structural differences with **3h**. Firstly, the CO ligand on the Fe(CO)(c-Hex-DAB) fragment is unambiguously semi-bridging in nature, with the Fe(2)···C(1) distance of 2.545(15) Å and the Fe(1)–C(1)–O(1) angle of 164.4(11)°. Secondly, the butadiendiyl moiety of the ferracycle is less strongly bonded to Fe(1). This is indicated by longer Fe(1)–C(ring) distances [Fe(1)–C(5): 2.120(16); Fe(1)–C(6): 2.140(14); Fe(1)–C(7): 2.123(16); Fe(1)–C(8): 2.134(15) Å], as well as by the bond lengths of the terminal C–C bonds [C(5)–C(6): 1.362(20) and C(7)–C(8): 1.380(21) Å] which are significantly shorter than the central C(6)–C(7) bond of 1.454(21) Å. These features may be explained by assuming less back-donation from Fe(1) into the anti-bonding π^* orbital of the butadiendiyl fragment.

Molecular Structure of $Fe_2[HC{=}C(H)C(H){=}CH]$-$(CO)_4$(i-Pr-DAB) (5)

Complex **5** may be regarded as the product of the substitution of the two terminal CO ligands in the plane of the ferracyle in $Fe_2[HC{=}CHCH{=}CH](CO)_6$ (**6**) by two N donor atoms of the chelating DAB ligand (see Fig. 6). It is therefore interesting to

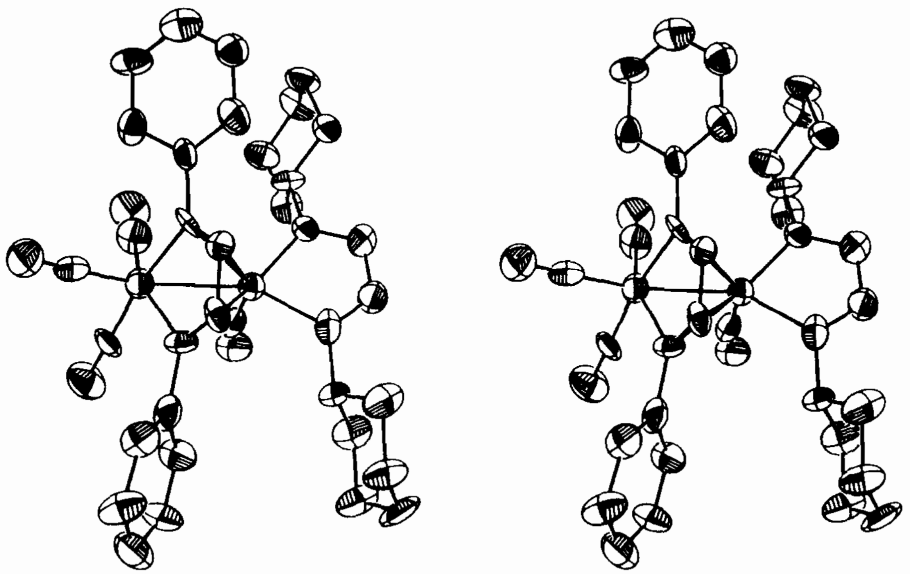

Fig. 5. Stereoscopic ORTEP representation of $Fe_2[PhC{=}C(H)C(H){=}CPh](CO)_4$(c-Hex-DAB) (3a) (ellipsoid probability scale: 36%).

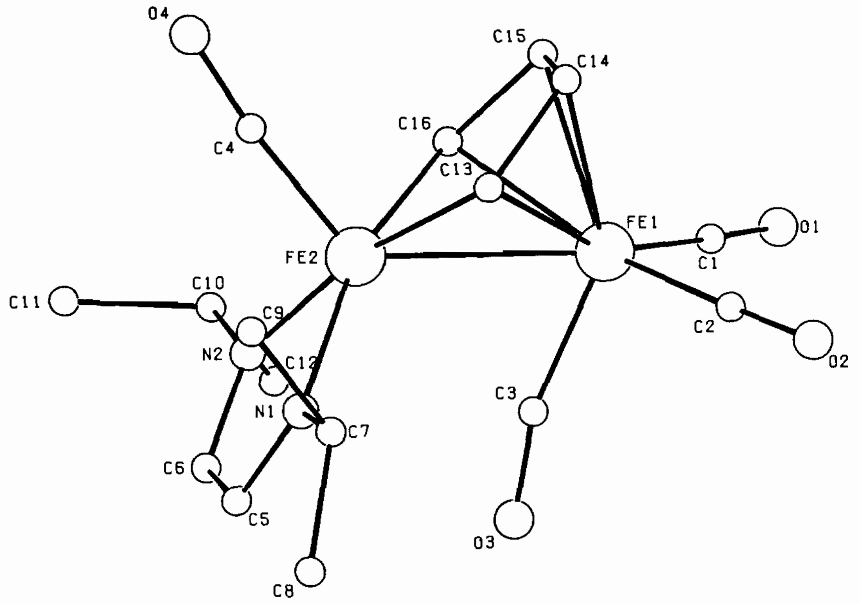

Fig. 6. PLUTO drawing of $Fe_2[HC{=}C(H)C(H){=}CH](CO)_4$(i-Pr-DAB) (5). The H atoms are omitted for clarity.

compare the molecular structure of 5 to that of 6, which was published by Dettlaf and Weiss in 1976 [25].

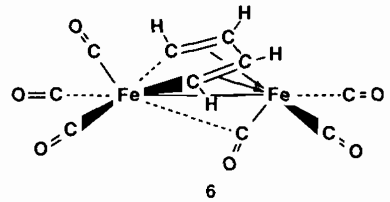

6

Complex 5 consists of an $Fe[HC{=}CHCH{=}CH]$-(CO)(i-Pr-DAB) fragment which is bonded to an $Fe(CO)_3$ unit via an Fe–Fe bond [Fe(1)–Fe(2): 2.541(3) Å] and the π-bonded butadiendiyl fragment [Fe(1)–C(13): 2.112(4); Fe(1)–C(14): 2.116-(4); Fe(1)–C(15): 2.111(4); Fe(1)–C(16): 2.115(4) Å]. One of the CO ligands on the $Fe(CO)_3$ moiety is semi-bridging [∠Fe(1)–C(3)–O(3): 165.8(3)°; Fe(2)...C(3): 2.501(4) Å]. These values are almost identical to those of 6 [∠Fe–C–O: 167.3(7)°; Fe...C: 2.508(4) Å]. There are, however, a number of different features. The terminal C–C bonds in **5** [C(13)–C(14): 1.426(5); C(15)–C(16): 1.427(6) Å] are longer than those of 1.368(9) and 1.409(6) Å in **6**, whereas the central C–C bond lengths are almost equal [1.411(7) Å in **5** *versus* 1.412(9) Å in **6**]. This is most likely the result of the presence of two hard N donor atoms *trans* to the butadiendiyl fragment. The redistribution of the resulting excess of electron density on Fe(2) in a π^* MO of the butadiendiyl fragment causes the elongation of the terminal C–C bonds. The shorter Fe(2)–C(4) bond distance of 1.718(5) Å and the longer C(4)–O(4) distance of 1.158(5) Å of the CO ligand on the Fe in the ferracycle in **5** with respect to the corresponding distances of 1.744(5) and 1.149(8) Å in **6** indicate that this CO is also involved in the redistribution of electron density donated by the DAB ligand. It is not quite clear how the longer Fe–Fe distance of 2.541(3) Å in **5** when compared to that of 2.515(1) Å in **6** has to be interpreted. The fact that the bonding geometry of the semi-bridging CO ligand going from **6** to **5** remains virtually unchanged suggests that the metal-d orbitals with which the DAB ligand in **5** interacts are not involved in the back-donation from Fe(2) into the semi-bridging CO. This is in contrast with 4e, for example, where instead of the two equatorial COs in **6**, onc equatorial CO and the axial CO are substituted by the R-DAB and where we do observe a markedly different bonding of the (semi-)bridging CO group.

NMR Spectroscopy

The ^{1}H and ^{13}C NMR data are listed in Tables 2 and 3, respectively. The NMR data of the reported compounds in solution are in agreement with the proposed molecular structures, which for three representative complexes are confirmed by solid state X-ray crystal structure determinations. The NMR spectra of the compounds of type **4** and those of **3f** and **3h–j′**, with the head-to-tail coupled alkynes or with L = R-Pyca, confirm the obvious absence of a symmetry plane in the molecules. The NMR spectra of the complexes **3** with L = R-DAB and two tail-to-tail coupled monosubstituted alkynes, indicate the presence of a symmetry plane in the molecule (defined by both Fe atoms, the semi-bridging CO and the center of the central C–C bonds of the DAB and butadienediyl ligands) in solution, causing the two halves of the molecule to be equivalent. This can be concluded from the single resonance observed for both imine protons, as well as for both alkyne CH protons. The molecular structure of **3a**, however, does not show an element of symmetry in the solid state. Since this is most likely not due to crystal packing effects we have to assume that in solution some fluxional process occurs, causing the two halves of the molecule to become equivalent on the NMR timescale. This process probably involves a small back and forth rocking of the Fe(CO)(R-DAB) unit with respect to the Fe(C_4R_4)(CO) unit along the Fe–Fe axis. This is probably a low energy process, since for **3a** only below 155 K at 250 MHz the singlet due to the alkyne protons at 6.64 ppm shows a splitting into two very broad signals. This corresponds with an activation energy of 30–35 kJ mol^{-1}.

IR Spectroscopy

The IR data (ν-CO region) in hexane or CH_2Cl_2 solution are listed in Table 3. The absorptions of the terminally bonded CO ligands are found as expected in the range of 1920–2060 cm^{-1}. The stretching frequencies of the ester carbonyl group in DMADC and MP derivatives are observed between 1740 and 1660 cm^{-1}. The absorptions due to the (a)symmetrically bridging CO in the type **4** complexes are found between 1770 and 1800 cm^{-1} for complexes derived from PTA, PHA or DPHA, and between 1810 and 1850 cm^{-1} for the complexes derived from DMADC or MP.

The stretching frequencies of the semi-bridging CO ligands in the complexes **3** are found between 1870 and 1940 cm^{-1}. Also the complexes **3** derived from DMADC or MP show an absorption due to the semi-bridging CO at significantly higher frequency when compared to the complexes derived from other alkynes. It seems reasonable to assume that this is due to an electronic effect. Since not only the frequencies of the (semi-)bridging COs are increased but also those of the terminally bonded ones, the most likely explanation is that the electron withdrawing effect of the methoxycarbonyl groups causes an overall decrease of backbonding from the Fe centers to the CO ligands, thus increasing their stretching frequencies.

UV–Vis and Resonance Raman Spectroscopy

The reported compounds are all intensely coloured, either dark purple (**3**) or brown (**4**). The UV–Vis spectrum of **3a**, Fe_2[PhC=CHCH=CPh]-$(CO)_4$(c-Hex-DAB), showed a strong band at 557 nm (ϵ = 8770) and a weaker one at 465 nm. The isomeric brown compound **4a** also showed two bands, one at 480 nm (ϵ = 4630) and one at 406 nm of about equal intensity.

In order to assign these absorption bands, resonance Raman (rR) spectra of **3a** and **4a** were recorded with different excitation laser lines. The rR spectrum of **3a** in benzene, obtained by excitation with λ = 569 nm, close to the maximum of its lowest energy band, shows rR effects for bands at 182(m), 320(m), 686(s), 961(m) and 1469(w) cm^{-1}. In agreement with other R-DAB complexes [26–33], the 1469 cm^{-1} band is assigned to ν_s(C=N) of this ligand. The 320 cm^{-1} band is assigned to ν_s(Fe–N), while the other bands belong to deformation modes of the Fe–R-DAB moiety. Changing the excitation wavelength to λ = 514.5 nm, at the high energy side of this band, caused, apart from the appearance of several new weak bands, a decrease of rR intensity for the low frequency bands and an intensity increase for the 1469 cm^{-1} band. Furthermore, a new band of medium intensity showed up at 451 cm^{-1} which is assigned to ν(Fe–C).

These results show that the 560 nm UV band of **3a** belongs to one or more electronic transitions within the Fe–R-DAB metallacycle. The large change in rR intensity upon going from 569 to 514.5 nm excitation, point to the presence of at least two transitions from different metal-d orbitals. Apparently, excitation with λ = 514.5 nm takes place into a transition with rather strong Fe → R-DAB charge transfer character, because of the strong rR effect observed for ν_s(C=N) at 1469 cm^{-1}. The high-energy band of **3a** is assigned to an Fe → R-DAB transition with an underlying LF transition which most probably takes place from a metal-d orbital involved in the back-bonding to the butadiendiyl fragment.

Complex 4a has two absorption bands in the visible region at 480 and 405 nm, respectively. The rR spectra, obtained by excitation into these bands were all very weak and only the 514.5 nm spectrum will be discussed here. Two bands show up in this spectrum, at 1513 (ν_s(C=N)) and 484 (ν_s(M–C)) cm^{-1}, respectively. Again, we are dealing with one or more Fe → R-DAB transitions within the low-energy band. No rR spectra could be obtained by excitation into the 405 nm band, because this is outside the wavelength region of our laser lines.

The low frequency of ν_s(C=N) of the R-DAB ligand in **3a** (1469 cm^{-1}) with respect to **4a** (1513 cm^{-1}) indicates a stronger π-back-bonding to the R-DAB ligand in the former complex. This result suggests a higher electron density at the Fe center π-bonded to the ferracycle in **3a** than at the Fe atom in the ferracycle in **4a**. It also explains the shift to lower energy of the MLCT band upon going from **4a**, in which the R-DAB is bonded to the Fe atom in the ferracycle to **3a** in which the R-DAB is coordinated to the Fe center which is π-bonded to the ferracycle.

Complex Formation

The question arises what determines the choice for the formation of ferracyclopentadienyl complexes of type 3 and/or type 4 in the reactions of $Fe_2(CO)_6(L)$ [L = R-DAB, R-Pyca] with alkynes. In one case it could be shown unambiguously that the type 4 complexes are formed via a dinuclear intermediate containing the first alkyne bonded as a 4e donor in the μ_2,η^2-perpendicular bridging position, *i.e.* the formation of **4e, f** via $Fe_2(CO)_5$(i-Pr-DAB)-[μ_2,η^2-MeOC(O)C≡CC(O)OMe] (2) (see eqn. (2)). This, however, does not prove that the formation of the type 3 complexes also proceeds via an intermediate of type 2. When we consider how the product distribution depends on the nature of both L and the alkyne, there is one obvious trend that can be noticed. In the case of the disubstituted alkynes (DPHA and DMADC) only compounds of type 4 are formed while type 3 complexes are only observed in the case of monosubstituted alkynes. Since DPHA and DMADC have similar steric demands but different electronic properties due to the much stronger electron withdrawing effect of the methoxycarbonyl substituents, their similar reactivity towards 1 suggests that the product distribution is mainly determined by steric factors. This latter conclusion is corroborated by the fact that only in the case of ethyne is a complex of type 5 formed. It seems not unlikely that when one or both of the terminal butadiendiyl C atoms C(13) and C(16), which are in one plane with N(1) and N(2), in 5 bear a substituent, there would be a strong destabilization due to steric interactions of these substituents with the DAB R-groups on the N atoms (see Fig. 1).

The formation of the ferracyclopentadienyl complexes from intermediate 2 may involve either a direct side-on attack of the second alkyne on the μ_2,η^2-bridging alkyne, as described by Thorn and Hoffmann [34], or via the substitution of one of the CO ligands by the second alkyne, after which the two coordinated alkynes are coupled to give the ferracycle.

Bonding Within the Complexes

An intriguing aspect of the reported compounds is the presence of CO ligands in various degrees of bridging positions, varying from asymmetrically bridging (**4e**), via semi-bridging (**3a** and **5**) to almost terminally bonded (**3h**). In the past decade several papers have appeared in the literature contributing to the discussion about the reasons of existence and bonding properties of the semi-bridging CO ligand in the dinuclear metallacyclopentadienyl complexes M_2[RC=CRCR=CR]$(CO)_6$ [22, 35, 36].

In order to understand the bonding of the (semi)-bridging CO ligands in the complexes reported in this paper we have to regard the influence of the chelating α-diimine ligand on the electron distribution within the complexes. In this discussion we will assume that, although both CO and α-diimine ligands have σ-donating as well as π-accepting capacity, the hard σ-N donor atom of an α-diimine ligand is a net electron donor when compared to a CO ligand, which is a net electron acceptor. A recent theoretical study of the electronic structure of some of the complexes reported in this paper has confirmed this assumption [36b].

In the complexes 4 with the α-diimine bonded to the Fe atom in the ferracycle, we observe an (a)symmetrically bridging CO, whereas in the compounds **3** with the α-diimine bonded to the other Fe center, a semi-bridging CO is present. Also **5** contains a semi-bridging CO. When we consider the metal–metal bond as a donor–acceptor interaction, we can rationalize this coordination behaviour using Cotton's theory [35a]. This theory concerns the bonding in the complexes $M_2[RC{=}CRCR{=}CR](CO)_6$, containing a $M(CO)_3[RC{=}CRCR{=}CR]$ metallacyclopentadienyl unit bonded to an $M'CO)_3$ unit of which one of the CO ligands is semi-bridging. The theory is based on the assumption of a dative $M' \rightarrow M$ metal–metal bond, which is necessary for both metal centers in the complex to obey the 18-electron rule, when the COs are all regarded as terminally bonded. To compensate for the resulting M^+–M^- polarization in the complex, a back-donation of electron density occurs from M into the π^*-orbital of one of the CO ligands on M′, which thus becomes semi-bridging. When two CO ligands of the Fe atom in the ferracycle in $Fe_2(C_4R_4)(CO)_6$ are replaced by a chelating α-diimine resulting in a type **4** complex, e.g. **4e**, the electron density donated by the N atoms of the α-diimine adds to the existing negative polarization of Fe(1) in the ferracycle. This makes an even stronger back-bonding from Fe(1) to the semi-bridging CO necessary, causing it to become (a)symmetrically bridging. The redistribution of the negative charge on the Fe atom can in contrast to **5** not proceed via back-donation to the DAB ligand, due to its bonding mode (*i.e.* one N atom in an equatorial and one N atom in an apical position, see Fig. 1) and can therefore only be achieved by back-donation to the bridging CO and the butadiendiyl ligand. This last observation is in agreement with the strong elongation of the terminal butadiendiyl C=C bonds (see above). When, however, we substitute in $Fe_2(C_4R_4)(CO)_6$ two COs on the other Fe by an α-diimine, as for example in **3h**, the α-diimine partly compensates for the positive polarization of the Fe bonded to the ferracycle and therefore decreases the relative negative polarization on the Fe in the ferracycle. Hence, less back-donation to the semi-bridging CO ligand is needed and it becomes more terminally bonded.

A combined theoretical and experimental investigation of the electronic structure of **5** showed that in this complex, in contrast to the complexes **3**, no dative Fe → Fe bond exists [36b]. Nevertheless in **5** a semi-bridging CO is present, which is necessary for a partial redistribution of the accumulated negative charge on the Fe center, caused by the σ-N donor atoms of the DAB ligand.

This leaves one aspect of the bonding within the reported type **3** complexes unexplained: the stronger π,π-bonding of the butadiendiyl fragment in **3h** (with two tail-to-tail coupled PHA molecules) when compared to **3a** (with two head-to-tail coupled MP molecules), combined with the more pronounced bridging character of the semi-bridging CO in **3a**, relative to **3h**. This may be due to the steric repulsion in **3h** between the isopropyl group on N(1) and the methoxycarbonyl group on C(7) which prevents a completely staggered configuration of the Fe(2)-$(CO)_3$ and Fe(1)(CO)(i-Pr-DAB) fragments. This hampers the possibility for C(4)O(4) to become semi-bridging, both because of the decrease in overlap between Fe(2) and C(4)O(4) and the steric repulsion between C(1)O(1) and C(4)O(4). The redistribution of electron density consequently has to proceed via the butadiendiyl moiety, which becomes more strongly bonded to Fe(1). This is corroborated by the elongation of the C(5)–C(6) and C(7)–C(8) bonds and the shortening of the Fe(1)–C(ring) bonds, when compared to **3a**. The reduced back-donation via the semi-bridging CO in **3h** is also compensated by a stronger back-bonding to the CO on Fe(2), perpendicular to the ferracycle. This is shown by the shorter Fe(2)–C(3) distance of 1.71(1) Å, when compared to the Fe(2)–C(1) and Fe(2)–C(2) bond lengths of 1.809(10) and 1.79(1) Å, respectively and by slightly longer C(3)–O(3) distance of 1.16(1) Å when compared to 1.14(1) Å for both C(1)–O(1) and C(2)–O(2). In **3a**, the Fe(2)–CO distances are about equal, which also applies for the C–O distances, indicating the absence of increased back-bonding. In **3a** there is no steric repulsion between the DAB ligand and the alkyne substituents, which results in a rotation of about 13° of the Fe(CO)(i-Pr-DAB) fragment relative to the $Fe(CO)_3$ fragment towards a staggered configuration when compared to the conformation of the corresponding fragments in **3h**. A second cause of a different bonding in **3a** and **3h** is that the electron withdrawing effect of the methoxycarbonyl groups in **3h** compensates for the excess of negative charge on Fe(2) and thus renders a semi-bridging CO less needed. The almost complete coplanarity of the C_4 unit and the atoms of the methoxycarbonyl substituents (r.m.s. deviation 0.07 Å) will indeed facilitate the delocalization over this organic fragment. The results of the above-mentioned theoretical study are supportive of this observation [36b].

Conclusions

It has been shown that dinuclear Fe carbonyl α-diimine complexes react with various alkynes to give ferracyclopentadienyl α-diimine complexes, in some cases among a number of other products. The formation of these products probably proceeds via an intermediate $Fe_2(CO)_5(L)[\mu_2,\eta^2$-alkyne] containing one alkyne molecule in a perpendicular bridging position. It has become clear that the nature of the α-diimine ligand has little influence on which type of ferracyclopentadienyl complex is formed but that its presence strongly influences the electron distribution and the bonding within the complexes. Whether the type **3** complexes with the α-diimine bonded to the Fe center bonded to the ferracycle or the type **4** complexes with the α-diimine bonded to the Fe atom in the ferracycle are formed depends more on the steric properties of the alkyne than on the electronic influences of the alkyne substituents. The observed coordination behaviour of the (a)symmetrically (in **4**) or semi-bridging (in **3** and **5**) CO ligands may be explained with the bonding model proposed by Cotton, although electron redistribution mechanisms involving the butadiendiyl fragment and the terminally bonded COs also seem to play an important role.

Supplementary Material

For **3a**: a table of anisotropic thermal parameters of the non-H atoms, a full listing of the bond lengths and angles of the non-H atoms and a listing of calculated *versus* observed structure factors (24 pages). For **3h**: a table of anisotropic thermal parameters of the non-H atoms, a table of the fractional coordinates and isotropic thermal parameters of the H atoms, a full listing of bond lengths and angles of all atoms, an ORTEP representation and a listing of calculated *versus* observed structure factors (12 pages). For **4e**: a table of anisotropic thermal parameters of the non-H atoms, a full listing of the bond lengths and angles of the non-H atoms, a stereoscopic ORTEP representation and a listing of calculated *versus* observed structure factors (14 pages). For **5**: a table of anisotropic thermal parameters of the non-H atoms, a table of the fractional coordinates and isotropic thermal parameters of the H atoms, a full listing of bond lengths and angles of all atoms, a stereoscopic ORTEP representation and a listing of calculated *versus* observed structure factors (23 pages). These can be ordered from the authors.

Acknowledgements

Mr J. M. Ernsting is thanked for assistance in measuring the ^{13}C NMR spectra. We are indebted to Dr C. H. Stam of the Laboratory for Crystallography of the University of Amsterdam for revising the crystal structure data. The Institute for Mass Spectrometry of the University of Amsterdam is thanked for measuring the FD mass spectra. Mr Th. L. Snoeck and Mr A. Terpstra are thanked for measuring the resonance Raman and UV–Vis spectra. Dr D. J. Stufkens is thanked for assisting in interpreting the UV–Vis and resonance Raman results. Dr H.-W. Frühauf and Dr C. J. Elsevier are thanked for critically revising the manuscript.

References

1 F. Muller, K. Vrieze, G. van Koten, D. Heijdenrijk, L. B. Krijnen and C. H. Stam, *Organometallics*, in press.

2 (a) G. van Koten and K. Vrieze, *Adv. Organomet. Chem., 21* (1982) 151; (b) K. Vrieze, *J. Organomet. Chem., 300* (1986) 307; (c) G. van Koten and K. Vrieze, *Recl. Trav. Chim. Pays-Bas, 100* (1981) 129; (d) G. van Koten and K. Vrieze, *Inorg. Chim. Acta, 100* (1985) 79.

3 J. Keijsper, P. Grimberg, G. van Koten, K. Vrieze, M. Christophersen and C. H. Stam, *Inorg. Chim. Acta, 102* (1985) 29.

4 (a) J. Keijsper, J. Mul, G. van Koten, K. Vrieze, H. C. Ubbels and C. H. Stam, *Organometallics, 3* (1984) 1732.

5 (a) G. van Koten, J. T. B. H. Jastrzebski and K. Vrieze, *J. Organomet. Chem., 250* (1983) 49; (b) L. H. Staal, A. Oskam, K. Vrieze, E. Roosendaal and H. Schenk, *Inorg. Chem., 18* (1979) 1634; (c) L. H. Staal, L. H. Polm, R. W. Balk, G. van Koten, K. Vrieze and A. M. F. W. Brouwers, *Inorg. Chem., 19* (1980) 3343; (d) L. H. Polm, G. van Koten, C. J. Elsevier, K. Vrieze, B. F. K. van Santen and C. H. Stam, *J. Organomet. Chem., 304* (1986) 353.

6 J. Keijsper, L. H. Polm, G. van Koten, K. Vrieze, J. D. Schagen and C. H. Stam, *Inorg. Chim. Acta, 103* (1985) 137.

7 L. H. Polm, G. van Koten, K. Vrieze, C. H. Stam and W. C. J. van Tunen, *J. Chem. Soc., Chem. Commun.*, (1983) 1177.

8 (a) L. H. Staal, G. van Koten, K. Vrieze, B. F. K. van Santen and C. H. Stam, *Inorg. Chem., 20* (1981) 3598; (b) F. Muller and K. Vrieze, in J. J. Ziolkowski (ed.), *Coordination Chemistry and Catalysis*, World Scientific Publ. Co., Singapore, 1988.

9 H.-W. Frühauf, A. Landers, R. Goddard and K. Krüger, *Angew. Chem., 90(1)* (1978) 56.

10 (a) W. Hübel, in I. Wender and P. Pino (eds.), *Organic Synthesis via Metal Carbonyls*, Vol. 1, Wiley Interscience, New York, 1968, p. 273; (b) W. P. Fehlhammer, H. Stolzenberg, in G. Wilkinson, F. G. A. Stone and E. Abel (eds.), *Comprehensive Organometallic Chemistry*, Vol. 4, Pergamon, Oxford, 1982, p. 549; (c) M. Chisholm, K. Folting, J. C. Huffman and N. S. Marchant, *Organometallics, 5* (1986) 602; (d) M. Leyendecker, W. S. Sheldrick and C. G. Kreiter, *J. Organomet. Chem., 270* (1984) C37; (e) R. P. Ferrari and G. A. Vaglio, *Gazz. Chim. Ital., 105* (1975) 939; (f) D. B. Pourreau, R. R. Whittle and G. L. Geoffroy, *J. Organomet. Chem., 273* (1984) 333; (g) S. Aime and A. J. Deeming, *J. Chem. Soc., Dalton Trans.*, (1981) 828; (h) S. Aime and E. Ochiello, *J. Chem. Soc., Dalton Trans.*, (1986) 1863.

11 B. L. Booth, R. N. Hazeldine and I. Perkins, *J. Chem. Soc., Dalton Trans.*, (1981) 2593.

12 T. L. Jacobs, in R. Adams (ed.), *Organic Reactions*, Vol. 3, Wiley, London, 1949, p. 1.

13 F. Muller, G. van Koten, K. Vrieze, D. Heijdenrijk, A. N. S. Mak, C. A. A. Duineveld and C. H. Stam, *Organometallics*, (1989), in press.

14 L. H. Staal, L. H. Polm and K. Vrieze, *Inorg. Chim. Acta, 40* (1980) 165.

15 F. Muller, I. M. Han, G. van Koten, K. Vrieze, D. Heijdenrijk, J. van Mechelen and C. H. Stam, *Inorg. Chim. Acta, 158* (1989) 99.

16 N. Walker, D. Stuart, *Acta Crystallogr., Sect. A, 39* (1983) 158.

17 J. M. Stewart, *The XRAY76 System, Tech. Rep. TR446*, Computer Science Center, Univ. of Maryland, College Park, MD, 1976.

18 D. T. Cromer and J. B. Mann, *Acta Crystallogr., Sect. A, 24* (1968) 321.

19 *International Tables for X-ray Crystallography*, Vol. 4, Kynoch Press, Birmingham, 1974.

20 A. R. Overbeek and H. Schenk, in H. Schenk, R. Olthoff-Hazakamp, H. van Koningsveld and G. C. Bassi, *Computing in Crystallography*, University Press, Delft, 1978.

21 A. A. Hock and O. S. Mills, *Acta Crystallogr., 14* (1961) 139.

22 R. Colton and M. J. McCormick, *Coord. Chem. Rev., 31* (1980) 1.

23 D. L. Thorn and R. Hoffmann, *Nouv. J. Chim., 3(1)* (1979) 39.

24 S. A. R. Knox, R. F. D. Stansfield, F. G. A. Stone, M. J. Winter and P. Woodward, *J. Chem. Soc., Dalton Trans.*, (1982) 173.

25 G. Dettlaf and E. Weiss, *J. Organomet. Chem., 108* (1976) 213.

26 R. W. Balk, D. J. Stufkens and A. Oskam, *Inorg. Chim. Acta, 28* (1978) 133.

27 R. W. Balk, Th. L. Snoeck, D. J. Stufkens and A. Oskam, *Inorg. Chem., 19* (1980) 3015.

28 R. W. Balk, D. J. Stufkens and A. Oskam, *J. Chem. Soc., Dalton Trans.*, (1982) 275.

29 P. C. Servaas, H. K. van Dijk, Th. L. Snoeck, D. J. Stufkens and A. Oskam, *Inorg. Chem., 24* (1985) 4494.

30 M. W. Kokkes, D. J. Stufkens and A. Oskam, *J. Chem. Soc., Dalton Trans.*, (1983) 439.

31 M. W. Kokkes, Th. L. Snoeck, D. J. Stufkens, A. Oskam, M. Christophersen and C. H. Stam, *J. Mol. Struct., 131* (1985) 11.

32 P. C. Servaas, W. C. de Lange, D. J. Stufkens and A. Oskam, to be published.

33 R. W. Balk, D. J. Stufkens and A. Oskam, *Inorg. Chim. Acta, 34* (1979) 267.

34 D. L. Thorn and R. Hoffmann, *Inorg. Chem., 17(1)* (1978) 126.

35 (a) F. A. Cotton, *Prog. Inorg. Chem., 21* (1976) 1; (b) A. Astier, J.-C. Daran, Y. Jeannin and C. Rigault, *J. Organomet. Chem., 241* (1983) 53; (c) M. Casarin, D. Ajo, G. Granozzi, E. Tondello and S. Aime, *Inorg. Chem., 24* (1985) 1241; (d) R. D. Adams, *J. Am. Chem. Soc., 102* (1980) 7476.

36 (a) M. Casarin, D. Ajo, A. Vittadini, D. E. Ellis, G. Granozzi, R. Bertoncello and D. Osella, *Inorg. Chem., 26* (1987) 2041; (b) R. Bertoncello, M. Casarin, M. Dal Colle, G. Granozzi, L. Mattogno, F. Muller, U. Russo and K. Vrieze, manuscript in preparation.